The chemistry of metal–organic frameworks for CO_2 capture, regeneration and conversion

Christopher A. Trickett[1–4], Aasif Helal[5], Bassem A. Al-Maythalony[6], Zain H. Yamani[5], Kyle E. Cordova[1–4,5] and Omar M. Yaghi[1–4,5]

Abstract | The carbon dioxide challenge is one of the most pressing problems facing our planet. Each stage in the carbon cycle — capture, regeneration and conversion — has its own materials requirements. Recent work on metal–organic frameworks (MOFs) demonstrated the potential and effectiveness of these materials in addressing this challenge. In this Review, we identify the specific structural and chemical properties of MOFs that have led to the highest capture capacities, the most efficient separations and regeneration processes, and the most effective catalytic conversions. The interior of MOFs can be designed to have coordinatively unsaturated metal sites, specific heteroatoms, covalent functionalization, other building unit interactions, hydrophobicity, porosity, defects and embedded nanoscale metal catalysts with a level of precision that is crucial for the development of higher-performance MOFs. To realize a total solution, it is necessary to use the precision of MOF chemistry to build more complex materials to address selectivity, capacity and conversion together in one material.

[1]*Department of Chemistry, University of California–Berkeley.*
[2]*Materials Sciences Division, Lawrence Berkeley National Laboratory.*
[3]*Kavli Energy NanoScience Institute at Berkeley.*
[4]*Berkeley Global Science Institute, University of California–Berkeley, Berkeley, California 94720, USA.*
[5]*Center for Research Excellence in Nanotechnology (CENT), King Fahd University of Petroleum and Minerals (KFUPM).*
[6]*King Abdulaziz City for Science and Technology – Technology Innovation Center on Carbon Capture and Sequestration (KACST–TIC CCS), KFUPM, Dhahran 31261, Saudi Arabia.*

Correspondence to O.M.Y.
yaghi@berkeley.edu

Reticular chemistry of metal–organic frameworks (MOFs) has emerged as a powerful tool for producing porous materials and precisely designing their interior to address the world's energy and environmental problems[1]. Of these, CO_2 capture and utilization stand out as particular challenges that the field of MOFs is well positioned to address[2,3]. Specifically, the chemistry of MOFs has been developed to the point that one can rationally and systematically modulate the interplay between the MOF structure and the desired properties. Over the past 25 years, four crucial developments have enabled MOFs to become promising candidates for CO_2 applications. The first is the invention and expansion of reticular chemistry — the design, functionalization and structural variation of porous, crystalline and extended solid materials[1]. A natural outcome of reticular chemistry is the realization of designable solids that serve specific end functions. Second, the marriage of molecular chemistry with framework chemistry has led to molecular-level control and atomically precise chemical transformations to be carried out within extended solids[4]. Third, the discovery of ultrahigh porosity and thus unprecedented surface areas has led to the real possibility of holding and compacting large quantities of gases in a confined space for extended periods of time. The fourth crucial development is the concept of 'heterogeneity within order',

whereby structurally and chemically different components are brought together to function synergistically within a framework[5].

With these concepts for structural design in hand, MOFs have been applied to the various components of the CO_2 cycle (FIG. 1). In the early years of the field, MOFs with large surface areas were used for CO_2 capture, concentration and ultimately storage and transport. For example, a gas cylinder filled with MOF-177 ($Zn_4O(BTB)_2$; BTB = 4,4′,4″-benzene-1,3,5-triyl-tribenzoate), a material with a Brunauer–Emmett–Teller (BET) surface area of 4,500 $m^2 g^{-1}$, can capture and store nine times the amount of CO_2 than the same gas cylinder without the MOF[6]. Following this, the tunability of the internal pore environment of MOFs has also been exploited to enhance the framework affinity towards selective CO_2 capture from mixed gas systems at low pressures (conditions typical for exhaust and flue gas streams)[2]. Once purified and concentrated, CO_2 can be used as a source for chemical feedstock. Indeed, MOF researchers have at their disposal the full arsenal of both molecular inorganic and organic reactivity to install chemically well-defined catalytic active sites either within or covalently attached to the MOF backbone structure. Remarkably, an extensive class of materials, supported by precision and well-developed molecular chemistry, has emerged as being capable of
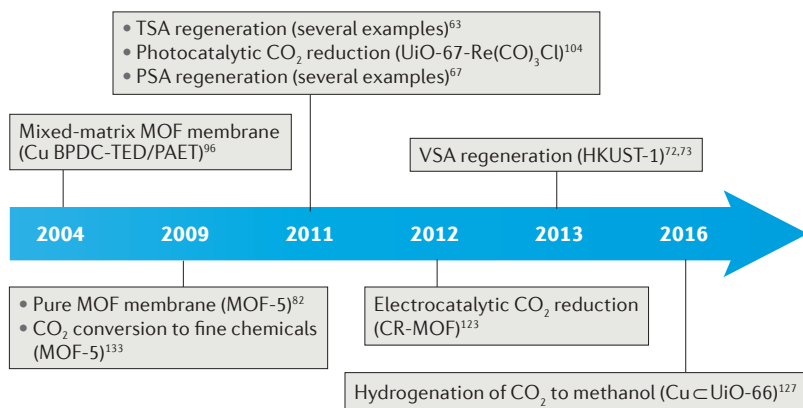
Figure 1 | **Chronology of key achievements made in the field of MOFs and CO_2.** Over the past two decades, significant discoveries have been made (and continue to be made) with respect to applying metal–organic frameworks (MOFs) to various components of the CO_2 cycle. PSA, pressure swing adsorption; TSA, temperature swing adsorption; VSA, vacuum swing adsorption; BPDC, biphenyl-4,4′-dicarboxylate; PAET, poly(3-acetoxyethylthiophene); TED, triethylenediamine.

effectively addressing the various major components of the carbon cycle (FIG. 1).

In this Review, we identify the structural and chemical features of MOFs that give rise to their most promising performance in the capture, regeneration and conversion of CO_2. We also evaluate the approaches used to employ MOFs at each stage of the CO_2 cycle and assess the relevance of these approaches to practical conditions.

Criteria for post-combustion CO_2 capture

A principle advance in the chemistry of CO_2 capture came with the development of reticular chemistry[1–3]. Indeed, the flexibility with which one can tailor a given MOF allows for the optimization and enhancement of CO_2 capture properties. The majority of research on developing MOFs for CO_2 capture has focused on reversible adsorption — a process that significantly lowers the need for energy input during regeneration and overcomes a key challenge of using traditional sorbents such as monoethanolamine solutions. As a result, the structures of MOFs have since been systematically developed, fine-tuned and studied in detail. In this section, we highlight important structural features that have been targeted in the development of MOFs for CO_2 capture under post-combustion conditions. These features, which are illustrated in FIG. 2, are: the presence of accessible coordinatively unsaturated metal sites in the pores; integration of heteroatoms within, as well as covalently linked functionality to, the backbone; specific interactions of MOF building units; hydrophobicity of the pores; and a hybrid of these structural features. We note that aside from the representative examples provided from each category discussed below, there exists a large body of research that could not be included. Accordingly, we report a comprehensive comparative summary, ranked by uptake, of all MOFs reported since 2012 for application in post-combustion CO_2 capture. We only include MOFs reported before 2012 in cases where such structures have the benchmark performance in a specific category (Supplementary information (sections 1,2; tables 1–10)).

Coordinatively unsaturated metal sites. MOFs endowed with coordinatively unsaturated metals take advantage of Lewis acidity, which is afforded by partial positive charges on metal sites. MOFs with these sites exhibit relatively high heats of CO_2 adsorption (Q_{st}) at low pressures, thus leading to substantial selectivity and CO_2 uptake. This is important when considering the case of CO_2 capture from flue gas: the larger quadrupole moment and greater polarizability of CO_2 compared with N_2 leads to a stronger electrostatic interaction with an exposed metal site. Accordingly, one of the most well-studied series of MOFs is M-MOF-74 ($M_2(2,5\text{-DOT})$; 2,5-DOT = 2,5-dioxidoterephthalate, M = Mg(II), Zn(II), Mn(II), Fe(II) and Ni(II), among others)[7–14]. The benchmark material in this series, Mg-MOF-74, has the highest uptake capacity (27.5 wt%) ever reported under standard conditions (298 K and 1 bar)[9]. The structure of M-MOF-74 comprises 1D secondary building units (SBUs) connected by 2,5-DOT linkers to form hexagonal channels that are ~12 Å in diameter. Each M ion is only five-coordinate following evacuation of the guest molecules, thus allowing the access and efficient binding of CO_2 (in an end-on manner) to the sixth coordination site. This binding mode for CO_2 is typically observed in MOFs containing coordinatively unsaturated metal sites[2]. The effectiveness of this structural feature in Mg-MOF-74 is highlighted by the high initial Q_{st} value of 47 kJ mol^{-1} (REF. 10). Although a study of breakthrough gas measurements found dynamic uptakes to correlate well with thermodynamic uptake measurements, exposure to moisture was shown to reduce the CO_2 uptake of the top-performing Mg-MOF-74 (REF. 15). This is because of competitive coordination of water molecules to the coordinatively unsaturated metal sites and is a real challenge to overcome when using MOFs with such structural features. Notwithstanding a major synthetic discovery to 'protect' the coordinatively unsaturated metal sites, there is little left to explore for this structural feature in realistic post-combustion CO_2 capture applications. However, as we elaborate in the following subsection, the coordinatively unsaturated metal sites can be exploited to tether heteroatoms that are capable of mitigating the problem of competitive water adsorption.

Heteroatoms. The incorporation of heteroatoms within the backbone or as part of a covalently bound functionality, especially those that possess high polarity and, in some cases, a nucleophilic nature, have shown great promise for offering strong interactions with CO_2. Aromatic amines are one such functionality that has been investigated. Using CAU-1 ($Al_4(OH)_2(OCH_3)_4(BDC\text{-}NH_2)_3 \cdot x H_2O$; BDC-$NH_2$ = 2-aminoterephthalate), a framework containing aluminium hydroxide clusters linked by BDC-NH_2, a moderate CO_2 uptake of 15 wt% at 298 K and 1 bar was achieved with an accompanying high initial Q_{st} value of 48 kJ mol^{-1} and CO_2/N_2 selectivity[16]. Heteroaromatic amines, in which non-coordinating nitrogen atoms are part of the aromatic ring and are thus free to interact with guest molecules, have also been investigated. An interesting example of a heteroaromatic amine is Zn(btz) (btz = 5-bis(5-tetrazolo)-3-oxapentane), which has a tetrazolate unit with two non-coordinating
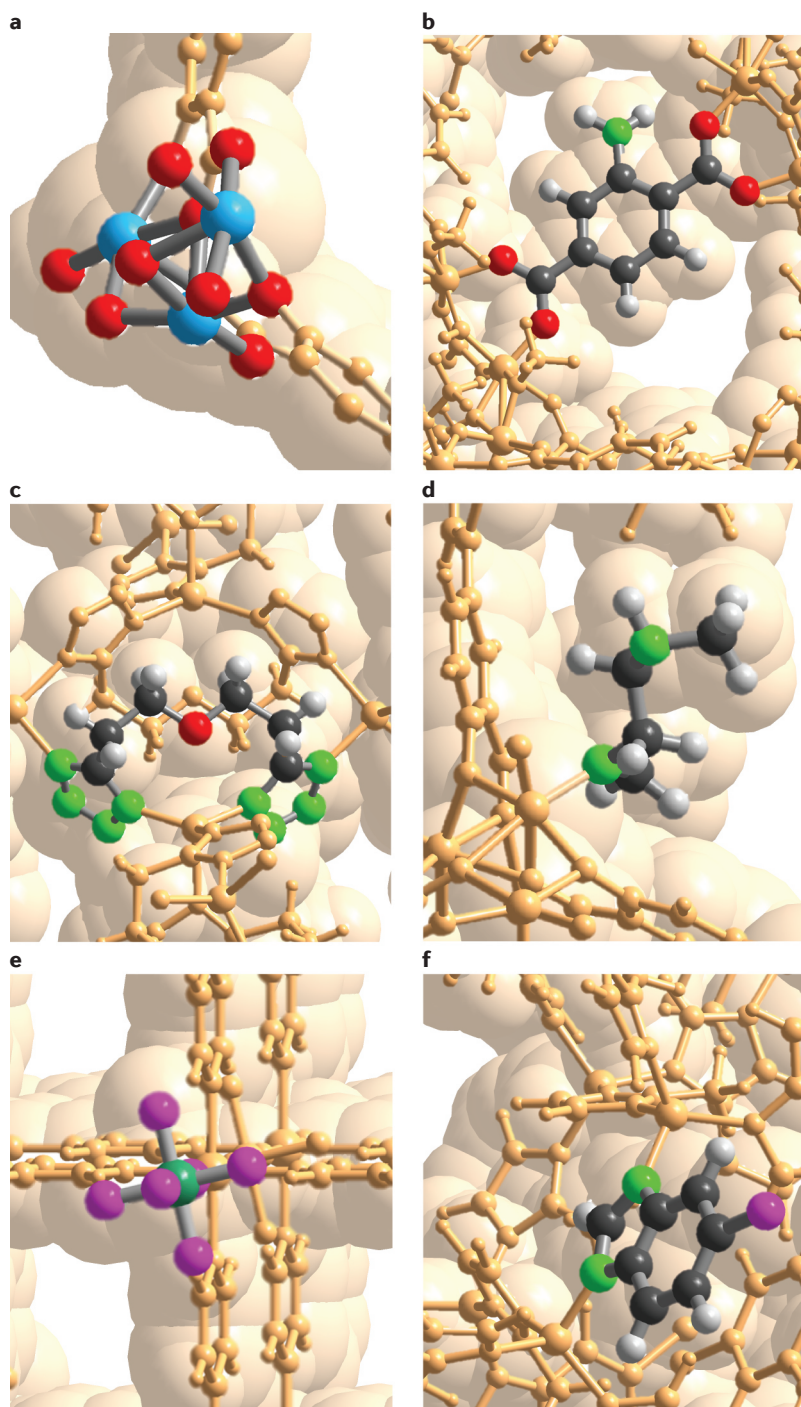
Figure 2 | **Important structural design features of effective MOF adsorbents for selective CO₂ capture. a** | Coordinatively unsaturated metal sites, as exemplified by the secondary building unit in Mg-MOF-74. **b** | Covalently linked polar functionalities, such as an aromatic amine in CAU-1. **c** | Heteroatomic amines, such as in Zn(btz) (btz = 5-bis(5-tetrazolo)-3-oxapentane), where non-coordinating N atoms are a component of the linker but are free to interact with CO₂. **d** | Alkylamines, either primary, secondary or tertiary, tethered to coordinatively unsaturated metal sites (for example, mmen-Mg-IRMOF-74-II; mmen = N,N-dimethylethylenediamine) or covalently bonded to the organic linker. **e** | Specific non-metallic interactions within the backbone (or pores) of a MOF structure (for example, SIFSIX-2-Cu-i (Cu(dpa)₂(SiF₆); dpa = 4,4′-dipyridylacety-lene)), which induce strong quadrupolar interactions with CO₂. **f** | Hydrophobicity and/or pore metrics for selectively capturing CO₂ in the presence of water (for example, ZIF-301). Colour code: C, black; O, red; N, green; F or Cl, purple; H, white; Si, dark green; and Mg, blue. The surrounding MOF structures are shown in pale orange.

nitrogen atoms. The resulting sodalite structure exhibits an uptake of 18 wt% CO₂ at 298 K and 1 bar (REF. 17). A method for further maximizing uptake is to use several types of heteroatomic sites within a single framework. In early work on heteroatoms, it was found that using adeninate (ad) as a linker to construct a 3D framework, termed bio-MOF-11 [Co₂(ad)₂(CO₂CH₃)₂], was a highly effective strategy for enhancing CO₂ uptake[18]. Adeninate has several different functionalities, including aromatic amine, pyrimidine and diazole groups, of which the latter two are involved as linkages in constructing the framework. We note that both the small pore size (5.8 Å) and the presence of internal pores containing both a free aromatic and heteroaromatic amine lead to a higher degree of interaction between the framework and CO₂. As a result of these structural features, bio-MOF-11 displayed an uptake of 15.3 wt% at 298 K and 1.1 bar, and a CO₂/N₂ selectivity of 75, as determined by ideal adsorbed solution theory[18,19].

The incorporation or grafting of dialkylamines within MOFs has also been proven as a promising approach to increase CO₂ uptake. The advantage of such systems is that CO₂ is adsorbed in a chemisorptive process, which typically leads to higher selectivity and uptake at pressures (1–2 bar) relevant to carbon capture from flue gas. In addition, alkylamine functionalities overcome the challenge of competitive adsorption of CO₂ in the presence of water. The first example of grafting dialkylamines in MOFs was reported in 2008 using MIL-101(Cr) (Cr₃(F,OH)(H₂O)₂O(BDC)₃·xH₂O; BDC = terephthalate) in which the amines are bound to Cr (REF. 20). However, the grafted material was not tested for CO₂ uptake at the time. In a subsequent report, ethylenediamine (en) was grafted onto Cu(II) in the structure of CuBTTri (H₃[(Cu₄Cl)₃(BTTri)₈]; BTTri = 1,3,5-tris(1H-1,2,3-triazol-5-yl)benzene)[21]. This structure is composed of Cu₄Cl SBUs linked by a tritopic triazolate with one non-coordinating nitrogen atom. It was found that the en-functionalized CuBTTri (1.6 wt% CO₂ uptake) outperforms the parent framework (0.92 wt%) at low pressure (~0.06 bar) and 298 K. This result is probably due to the much higher Q_{st} value (~90 kJ mol⁻¹) of the dialkylamine-functionalized material, which was in stark contrast to the Q_{st} value (20 kJ mol⁻¹) of the unfunctionalized parent CuBTTri. A follow-up report demonstrated how a stoichiometric amount of N,N-dimethylethylenediamine (mmen), a secondary amine, could be tethered to the Cu(II) atoms of the SBU to enhance CO₂ uptake to 15.4 wt% at 298 K and 1 bar, corresponding to 15% higher uptake than the original material. The mmen-functionalized CuBTTri exhibited a CO₂/N₂ selectivity of 327 at 0.15 bar CO₂, 0.75 bar N₂ and 298 K, as calculated by ideal adsorbed solution theory. Again, the Q_{st} value was very high (96 kJ mol⁻¹), indicating a chemisorptive process[22]. The coordinatively unsaturated metal sites of Mg-IRMOF-II (Mg₂(dobpdc); dobpdc = 4,4′-dioxido-3,3′-biphenyldicarboxylate) have also been exploited for grafting mmen (REF. 23). It was shown that mmen-Mg-IRMOF-74-II has an uptake of 14.5 (12.1) wt% CO₂ at 1 (0.1) bar and 298 (313) K with a high Q_{st} value of 71 kJ mol⁻¹.

Although grafting of dialkylamines has proven effective in increasing the uptake and selectivity of CO_2 under dry conditions, it was not until 2014 that this strategy was extended to assess the performance of MOFs under more realistic humid conditions. This was a natural progression as alkylamine-functionalized frameworks form covalent bonds with CO_2 and not with water. Accordingly, the organic linker of the expanded version of Mg-MOF-74, known as Mg-IRMOF-74-III ($Mg_2(DH3PhDC)$; DH3PhDC = 2′,5′-dimethyl-3,3″-dihydroxy-[1,1′:4′,1″-terphenyl]-4,4″-dicarboxylate), was covalently functionalized with a range of aromatic, primary, secondary and tertiary amines and tested for its CO_2 capture properties under wet flue gas conditions[24] (FIG. 3). Of these functionalized frameworks, the most effective was found to be the primary alkylamine, with an uptake of 12.7 wt% at 298 K and 1.1 bar. Dynamic breakthrough experiments showed no difference in the performance of this material under dry or wet (65% relative humidity) conditions, whereas that of the methyl-functionalized control experiment showed a loss of 80% in capacity under wet conditions. Although this discovery is promising for the selective capture of CO_2 in the presence of water, the achieved uptake falls short of the top-performing materials (albeit under dry conditions). Thus, the future of using heteroaromatic amine groups for CO_2 capture in MOFs lies in increasing the density of alkylamines within the framework.

Other heteroaromatic functional groups, such as imines and amides, have been used with varying degrees of success[25,26]. For example, linkers comprising amide moieties are conspicuous because of their rigidity and potential for increasing the affinity of the framework towards CO_2. However, it was recently shown that the preferential CO_2 binding sites in the amide-containing framework MFM-136 [$Cu(C_{19}H_{11}N_3O_5)(H_2O)_3$] were dominated by multiple phenyl rings on the linker, as opposed to the amide functionalities themselves[27]. This is not to say that CO_2 has no interaction with amide units; rather, it merely suggests that the CO_2–amide interaction is a minor contributor in amide-based MOFs with high CO_2 uptake. Indeed, there is a continued need for a deeper experimental understanding of framework–CO_2 interactions to determine the structural features responsible for strong CO_2 adsorption performance.

SBU-based interactions. Similar to the partial positive charge of a coordinatively unsaturated metal, strong interactions with CO_2 can be induced with non-metallic functional groups that are part of the SBU. This is observed for the frameworks SIFSIX-1-Cu ($Cu(4,4′-bpy)_2(SiF_6)$; 4,4′-bpy = 4,4′-bipyridine) and SIFSIX-2-Cu-i ($Cu(dpa)_2(SiF_6)$; dpa = 4,4′-dipyridylacetylene), which display CO_2 uptake capacities of 19.1 and 19.2 wt% at 298 K ambient pressure, respectively — the highest uptake reported for a MOF without coordinatively unsaturated metal sites[28,29]. More recently, the use of monodentate hydroxide moieties as capping ligands was demonstrated to be effective for strongly adsorbing CO_2 in the presence of water[30]. Specifically, a series of isostructural MOFs, MAF-X25 ($Mn^{II}_2Cl_2(bbta)$; bbta = $1H,5H$-benzo($1,2-d$:$4,5-d′$)bistriazolate), MAF-X25ox [$Mn^{II}Mn^{III}(OH)Cl_2(bbta)$], MAF-X27 [$Co^{II}_2Cl_2(bbta)$], and MAF-X27ox [$Co^{II}Co^{III}(OH)Cl_2(bbta)$], showed that by introducing an exposed monodentate hydroxide, the CO_2 adsorption increased by up to 50% relative to the parent MOF structure. Owing to the strong, selective binding of CO_2, MAF-X27ox exhibited no loss in dynamic CO_2 uptake under dry or humid conditions[30]. However, further investigations are needed to determine whether these frameworks with such SBU-based interactions are recyclable under actual flue gas conditions, which will assess their ability to withstand prolonged use for CO_2 capture.

Hydrophobicity. Although polar functional groups have the advantage of stronger interactions with CO_2 as a method of increasing both uptake and selectivity, installing hydrophobicity is an alternative for the capture of CO_2 by simple exclusion of water from the pores. The hydrophobic series of zeolitic imidazolate frameworks (ZIFs), ZIF-300 ($Zn(2-mIm)_{0.86}(bbIm)_{1.14}$; 2-mIm = 2-methylimidazolate, bbIm = 5(6)-bromobenzimidazolate), ZIF-301 ($Zn(2-mIm)_{0.94}(cbIm)_{1.06}$; cbIm = 5(6)-chlorobenzimidazolate) and ZIF-302 ($Zn(2-mIm)_{0.67}(mbIm)_{1.33}$; mbIm = 5(6)-methylbenzimidazolate), demonstrated that CO_2 uptake is equally effective under dry conditions and in the presence of 80% humidity[31]. In addition, these ZIFs were proven to be recyclable over three consecutive trials without loss of performance, which is an added benefit of using hydrophobic frameworks. Alternatively, post-synthetic modification is a useful tool for introducing hydrophobicity within a MOF material. In one such case, polynapthylene (PN) was formed within MOF-5 [$Zn_4O(BDC)_3$] by first loading the pores with 1,2-diethynylbenzene monomers.
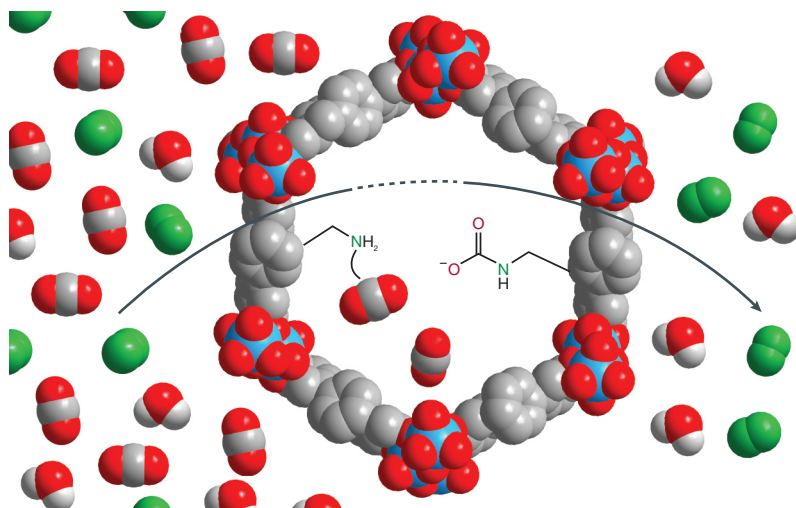

Figure 3 | **IRMOF-74-III with alkylamine functionality for the chemisorption of CO_2 in the presence of water.** The structure of Mg-IRMOF-74-III or $Mg_2(DH3PhDC)$ is depicted in space-filling form. Lining the pore walls of Mg-IRMOF-74-III is a covalently linked alkylamine functionality that, when exposed to CO_2, reacts to form a carbamate. This occurs even in the presence of nitrogen gas and water vapour. Colour code for space-filling form: C, grey; O, red; and Mg, blue. Colour code for guest molecules: C, grey; O, red; H, white; and N, green. DH3PhDC, 2′,5′-dimethyl-3,3″-dihydroxy-[1,1′:4′,1″-terphenyl]-4,4″-dicarboxylate.

Through heating, a Berman cyclization and subsequent radical polymerization occurred to afford polynapthylene. As a consequence, the PN⊂MOF-5 material doubled the CO_2 capacity, increased the CO_2/N_2 selectivity by a factor of about 25 and maintained >90% CO_2 capacity under humid conditions[32,33].

In general, MOF materials that solely rely on hydrophobicity for the selective capture of CO_2 over water suffer from poor uptake (owing to a lack of strong CO_2 binding sites) in comparison with MOFs with other structural features. Although hydrophobic frameworks are a significant step in the right direction for applying MOFs under practical conditions, there remains a noticeable absence in combining all positive structural features within one material. The future for hydrophobic MOFs involves the design of such a framework with coordinatively unsaturated metal sites or heteroatoms, which are shielded from water by the hydrophobicity of the framework.

Hybrid approaches. The goal of hybrid systems is to maximize the density of strong binding sites that promote strong interactions with CO_2. The best examples of this approach are MOFs constructed from Cu(II) SBUs with a triazole linker that has non-coordinating nitrogen atoms[34], JLU-Liu20 (Cu_6(TADIPA)_3(DABCO); TADIPA = 5,5′-(1H-1,2,4-triazole-3,5-diyl)diisophthalate, DABCO = 1,4-diazabicyclo[2.2.2]-octane) and JLU-Liu21 [Cu_6(TADIPA)_3(H_2O)_6]; a triazole- and pyridine-containing linker[35], (Cu(Me-4py-trz-ia); Me-4py-trz-ia = 5-(3-methyl-5-(pyridin-4-yl)-4H-1,2,4-triazol-4-yl)isophthalate); a triazine linker in CuTDPAT (Cu_3(TDPAT)(H_2O)_3; TDPAT = 2,4,6-tris (3,5-dicarboxylphenylamino)-1,3,5-triazine)[36] or CuTATB-60 (Cu_6(H_2O)_6(TATB)_4; TATB = 4,4′,4′′-s-triazine-2,4,6-triyl-tribenzoate)[37]; and by including amide functionalities as part of the linker backbone[38]. Finally, a mixed linker MOF, $Zn_2(tdc)_2(MA)$ (tdc = 2,5-thiophenedicarboxylate, MA = melamine), containing a Zn(II) paddlewheel cluster, dangling aromatic and heteroaromatic amines, as well as a thioether group, was shown to exhibit an exceptionally high uptake (27.0 wt%) at 298 K and 1 bar, although the specific binding sites have yet to be identified[39]. The hybrid approach has led to MOFs that possess the structural features identified to give high capacity. Although such structures exhibit notable CO_2 uptake, their performance has not been assessed in the presence of water and under dynamic separation conditions. This is not as much a design problem as it is a lack of full evaluation and application of the materials.

CO₂ capture from air and natural gas

CO₂ capture in confined environments. Certain environments involving the transport of humans in a confined space present their own challenges in the build-up of CO_2 due to respiration. Over time, CO_2 build-up in sealed spaces, such as spacecraft and submarines, can adversely affect their occupants. Rising concentrations of CO_2 in these environments have been linked to headaches and lethargy, which has prompted a safe exposure limit of 1% CO_2 to be imposed[40]. However, the capture of

low-concentration CO_2 represents a significant challenge because of the difficulty in designing materials with sufficiently strong interactions at low coverage without the need for a large energy input for regeneration[41]. Recently, NbOFFIVE-1-Ni [NiNbOF_5(pyrazine)_2·2H_2O], containing 2D Ni(II) pyrazine layers intercalated with $(NbOF_5)^{2-}$ anions, was shown to be a viable material for this application[42]. As a result of the polar pore walls (inducing strong interactions) and ideally sized square channels (which are perfect pockets for CO_2 adsorption), NbOFFIVE-1-Ni was able to adsorb 8.2 wt% CO_2 under dynamic breakthrough conditions with 1% CO_2 in dry N_2. We note that the uptake reduced to 5.6 wt% under 75% relative humidity[42]. Although other MOFs, which have been functionalized with dialkylamines[23,24], outperform NbOFFIVE-1-Ni under these conditions, the lower energy input needed for regenerating NbOFFIVE-1-Ni is an attractive feature for the uptake of low-concentration CO_2 uptake. There is a vast space to explore for designing new materials with higher capacity than NbOFFIVE-1-Ni, while keeping in mind the key structural features that make this MOF promising.

CO₂ capture for natural gas upgrading. The separation of CO_2 from CH_4 is an important process for natural gas sweetening because CO_2, in the presence of moisture, is corrosive and lowers the energy efficiency[43,44]. Typically, the same structural features of MOFs used for post-combustion CO_2 capture apply here with the added advantage of exploiting the different kinetic diameters of CO_2 (3.3 Å) and CH_4 (3.8 Å) by adjusting the pore size[45]. Among the best performers is UTSA-49 (Zn(mtz)_2; mtz = 5-methyl-1H-tetrazolate) with a reported selectivity of 33.7 at 298 K for an equimolar mixture of CO_2 and CH_4 (REF. 46). The key features of this tetrazolate framework are the uncoordinated heteroaromatic nitrogen atoms and two types of small pore openings (2.9 Å × 3.6 Å and 3.6 Å × 4.0 Å), both of which favour CO_2 uptake over CH_4. Recently, a mixed-metal ZIF, ZIF-204 (Zn_2Cu_3(Im)_10; Im = imidazolate), was proven to be effective for selectively capturing CO_2 from a ternary gas mixture of CO_2, CH_4 and H_2O — conditions that are practical for biogas sources[47]. In this report, the dynamic CO_2 capacity was relatively small (1.6 wt%), yet the presence of water did not negatively impact the performance of the material. Furthermore, two polymorphic MOFs, Qc-5-Cu-α and -β [Cu(quinoline-5-carboxylate)_2], were constructed and demonstrated to be capable of size-selectively adsorbing CO_2 even in a humid environment. This is an interesting discovery because the pore size was tailored to promote molecular sieving of CO_2 over CH_4 (REF. 48). Many studies have focused on using different functional groups and structural features of MOFs for enhancing the CO_2/CH_4 selectivity, including coordinatively unsaturated metal sites[10], hydroxyl groups[49] and ionic frameworks[50].

Because MOF-based separations are maturing to the point that the water challenge for selective CO_2 capture is now being addressed, the next phase must certainly focus on the removal of other problematic natural gas impurities, such as H_2S. To date, there are relatively few reports detailing the stability of MOFs in the presence

of H_2S, let alone the selective capture of CO_2 in the presence of H_2S (REFS 51–54). Surely, this is the next grand challenge to overcome before the full implementation of MOFs as a solution for natural gas upgrading.

Short-term CO_2 storage and transport
Although the most desirable outcome for the capture and purification of CO_2 is its use by the chemical industry as a starting material, it is unrealistic to expect more than a small fraction of anthropogenic CO_2 to be recycled with such large quantities being produced annually. Thus, the question of how to store and, potentially, transport CO_2 arises. In this brief section, we focus our attention on those MOFs that have been evaluated for their potential in CO_2 short-term storage. The most important feature for this application is an ultrahigh uptake at elevated pressures (10–50 bar). Generally, the most successful MOFs demonstrate extremely high BET surface areas of 4,000–7,000 $m^2 g^{-1}$ (REFS 55–62), with many also possessing coordinatively unsaturated metal sites. The latter are successful for CO_2 storage because competition for adsorption with water is absent. The highest reported gravimetric uptake is 74.2 and 73.9 wt% at 298 K and 50 bar for MOF-200 ($Zn_4O(BBC)_2$; BBC = 4,4′,4″-(benzene-1,3,5-triyl-tris(benzene-4,1-diyl))tribenzoate) and MOF-210 (($Zn_4O)_3(BTE)_4(BPDC)_3$; BTE = 4,4′,4″-(benzene-1,3,5-triyl-tris(ethyne-2,1-diyl)) tribenzoate, BPDC = biphenyl-4,4′-dicarboxylate), respectively[62]. However, with other methods of CO_2 storage, such as carbon capture and sequestration technologies that offer immense storage capacity at low cost, the use of MOFs for long-term storage is considered impractical at present.

CO_2 regeneration
A full CO_2 capture process requires the design of an integrated capture and release process that enables efficient regeneration of the material and subsequent processing of CO_2 (that is, injection, storage or further utilization)[63]. An ideal process for regeneration must involve minimal energy input to remove the vast majority, if not all, of the CO_2 adsorbed and result in no degradation in performance. To this end, the weaker the binding energy of CO_2, the more efficient the release process will be, because this requires less energy and results in the least disturbance to the framework. Current technologies for the regeneration of the adsorbent materials have focused on pressure swing adsorption (PSA), vacuum swing adsorption (VSA) and temperature swing adsorption (TSA)[64,65].

In PSA and VSA, CO_2 is adsorbed at a given pressure and released by lowering the pressure. The difference between the two methods is that in a VSA process, CO_2 is adsorbed at close to ambient pressure, whereas PSA uses elevated pressures, typically ranging from 8 to 28 bar (REF. 66). Because pre-combustion flue gas streams are pressurized, PSA is better suited for CO_2 separation in the pre-combustion stage, whereas VSA is applicable for ambient pressure post-combustion streams. PVSA is a hybrid of both systems, with an elevated input pressure and a desorption pressure below ambient pressure. Early work on the use of PSA for MOFs was performed

on CuBTTri, Mg-MOF-74, MOF-177, Be-BTB [$Be_{12}(OH)_{12}(BTB)_4$] and Co(BDP) (BDP = 1,4-benzenedipyrazolate) by measuring the single-component isotherms of CO_2 and H_2 up to 40 bar (REF. 67). The MOFs with coordinatively unsaturated metal sites, namely CuBTTri and Mg-MOF-74, exhibited the highest working capacities and also outperformed zeolite 13X and activated carbon. Subsequent efforts were made to simulate an industrial PSA process using a pelletized form of MIL-53(Al) [Al(OH)(BDC)][68,69]. With a flow of 87% CH_4 and 13% CO_2, 92.8% of the methane input was recovered at a purity of 99.4% at 4 bar and 303 K, with a desorption pressure of 0.1 bar.

TSA is another common method for material regeneration by heating the adsorbent to drive off adsorbed molecules[63,70]. In general, porous solids (<2 $J g^{-1} K^{-1}$) have the advantage of much lower heat capacities than conventional monoethanolamine solutions (3–4 $J g^{-1} K^{-1}$, depending on concentration), which makes the TSA process attractive. In the case of MOFs, MOF-177 and MOF-74 (REF. 71) have both been evaluated for their ability to be regenerated by TSA[63].

To date, there have been relatively few studies regarding the regeneration of MOFs using a VSA system. In early work, VSA was shown to be inefficient with HKUST-1 ($Cu_3(BTC)_2$; BTC = 1,3,5-benzenetricarboxylate) when compared with TSA. This was attributed to the unsuccessful regeneration of the coordinatively unsaturated metal sites[72]. In a different study, HKUST-1 was exposed to a feed of 13–16% CO_2 in dry N_2 at 2 bar and 308 K, with desorption occurring at 0.15 bar. From this, the working capacity of HKUST-1 was 2.22 mmol g^{-1} with 63% CO_2 recovery[73]. In another study, UiO-66 [$Zr_6O_6(OH)_4(BDC)$] was investigated as an adsorbent for a PVSA process under both dry and wet simulated flue gas mixtures[74]. The conditions used included pressurizing the inlet gas to 2 bar at 328 K with 15% CO_2 and 9% moisture and desorption at 0.15 bar. However, only low purity (~60%) CO_2 was collected and there was a 25% drop in CO_2 capacity when moisture was present.

CO_2 separation by MOF membranes
The use of membranes for gas separation technologies has gained attention as an alternative to pressure, temperature and/or vacuum swing adsorption because it has lower energy consumption and infrastructure costs in conjunction with easier modes of operation[75]. Historically, polymers have been used owing to their low production costs, mechanical flexibility and ease of processability[76]. However, polymeric membranes suffer from short lifetimes and limited thermal and chemical stability[77]. When polymeric membranes are applied to the separation of CO_2 under flue or natural gas conditions, it is difficult to avoid plasticization of the polymers and a trade-off arises between achieving high permeability versus high selectivity[78,79]. MOFs have increasingly been viewed as a viable material for use in membrane-based gas separation processes owing to their capability in overcoming the challenges presented by polymeric membranes[80]. Indeed, considerable achievements have been made using MOF-based

membranes for increasing both the selectivity and permeability parameters in CO_2-containing gas separation processes, as illustrated in FIG. 4.

Pure MOF membranes. In 2005, the first synthesis of a pure MOF-5 thin film was reported, in which a bottom-up approach was used. In this study, nucleation of the MOF-5 crystals occurred on self-assembled organic monolayers, terminated by carboxylic acid functional groups that were attached to a Au(111) substrate[81]. However, it was not until 2009 that a MOF-based membrane (MOF-5 on porous alumina) was fabricated and proven to be capable of being used for the separation of gases[82]. Accordingly, single-component gas permeation studies demonstrated that the diffusion of simple gases (CO_2, H_2, CH_4, N_2 and SF_6) follow Knudsen diffusion behaviour (that is, pore size is comparable to the size of these gas molecules)[83]. In another study, a uniformly distributed ZIF-8 [$Zn(2\text{-}mIm)_2$] membrane was solvothermally synthesized on a $ZnAl\text{-}NO_3$-layered double hydroxide layer grown on a porous alumina substrate. This composite membrane achieved a CO_2/CH_4 separation factor that is indicative of a molecular-sieving mechanism. Furthermore, it was reported that the permeance of CO_2 in the CO_2/CH_4 mixture was higher than for that found in the CO_2 single-component gas stream[84]. The separation of CO_2 from H_2 was demonstrated using the 2D framework $Zn_2(bIm)_4$ (bIm = benzimidazolate) exfoliated to 1 nm thickness[85].

This ultrathin membrane achieved high permeance while still accomplishing a high selectivity of >200 at 393 K and 1 bar for a 1:1 mixture of CO_2 and H_2. This selectivity was attributed to size exclusion, because only H_2 can penetrate a defect-free material.

The advantages of using MOFs for such applications do not solely originate from their structural features. Rather, by using different synthetic techniques, a continuous membrane can be grown in a highly-orientated manner towards a specific channel that affords beneficial properties. In 2011, this idea was realized when a continuous membrane of ZIF-69 (Zn(cbIm)(nIm); nIm = 2-nitroimidazolate) was synthesized on a porous alumina substrate through a secondary seeded-growth method, in which the interstitial gaps were closed during secondary growth of the crystals[86]. The authors found that, with the help of a previous study[87], ZIF-69 could be synthesized in a highly-orientated manner along its *c* axis. This led to 1D channels with 7.8 Å pore openings that were perpendicular to the substrate. Binary gas permeation studies on equimolar gas mixtures of CO_2/ CH_4 and CO_2/N_2 demonstrated that both the selectivity (separation factors of 6.3 and 4.6 for CO_2/N_2 and CO_2/CH_4, respectively) and permeations (103.4 and 102.3×10^{-9} mol m^{-2} s^{-1} Pa^{-1} for CO_2/N_2 and CO_2/CH_4, respectively) of CO_2 are higher than those found for the single-component permeation.

In 2012, the secondary seeded-growth method was used to fabricate continuous bio-MOF-1 [$Zn_8(ad)_4(BPDC)_6O\cdot 2Me_2NH_2$] membranes supported on porous stainless steel substrates[88,89]. In this report, various levels of bio-MOF-1 layering were studied to compare the separation performance as a function of membrane thickness[89]. The three-layered bio-MOF-1 membrane was found to have the highest CO_2 permeance (11.9×10^{-7} mol m^{-2} s^{-1} Pa^{-1}) and CO_2/CH_4 selectivity (2.6). In a continuation of this work, the secondary seeded-growth method was later used to synthesize continuous membranes of bio-MOF-13 [$Co_2(ad)_2(butyrate)_2$] on porous alumina substrates[90]. The rationale for using bio-MOF-13 was based on its small pore sizes (3.2–6.4 Å), high surface area and attractive CO_2 uptake capacity. The separation performance of the resulting membrane was shown to have high CO_2 permeance (10^{-6} mol m^{-2} s^{-1} Pa^{-1}) leading to CO_2/CH_4 separation selectivities of 3.1–3.8. The separation performance was near the upper bound for polymeric membranes when included in the revisited (2008) Robeson plot[78] (FIG. 4).

More recently, a breakthrough was reported for the synthesis of a continuous, anionic zeolite-like MOF, sod-ZMOF-1 (In(ImDC)$_2$($C_3N_2H_5$)]·(DMF)$_x$; ImDC = imidazoledicarboxylate, DMF = N,N-dimethylformamide), membrane[91]. Through gas mixture permeation measurements, mimicking the conditions of both flue and natural gas, the permeation selectivity towards CO_2 was determined to be 10.5 and 4, respectively. These findings were rationalized as adsorption-driven permeation behaviour that resulted from the anionic nature of the framework in conjunction with the relatively small pore size (4.1 Å) of the MOF. Nevertheless, there has been an increasing number of reports of new pure
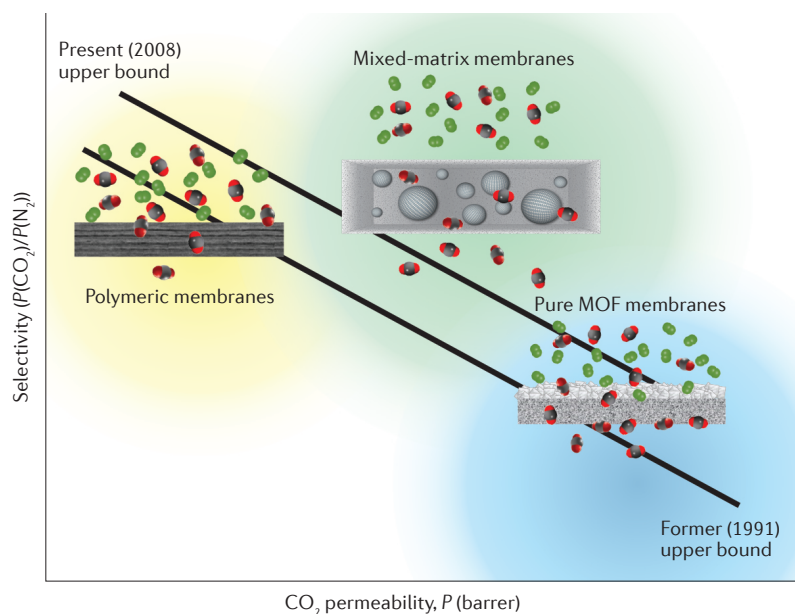

Figure 4 | **Selectivity versus CO_2 permeability compared to the Robeson upper bound curves for pure polymeric, mixed-matrix and pure MOF membranes.** The relationship between the CO_2/N_2 gas pair selectivity and CO_2 permeability is compared to the Robeson upper bound curves for pure polymeric membranes, mixed-matrix membranes and pure metal–organic framework (MOF) membranes. The general trend is increased selectivity towards CO_2/N_2 with the use of mixed-matrix membranes (shown with MOF nanoparticles embedded within) and increased permeabilities for pure MOF membranes (shown on a porous substrate) when compared to traditional polymeric membranes. Each membrane depicts the separation of CO_2 from a gaseous mixture containing N_2. Colour code for gas molecules: C, grey; O, red; and N, green.

MOF or ZIF membranes that target CO_2 separation[92–95] (Supplementary information (section 3; tables 11,12)).

In general, MOFs that combine a small pore aperture (within the range of the kinetic diameter of the target gas) with relatively high CO_2 affinity are the best candidates for use in membrane-based separations. This is primarily owing to the fact that small apertures and high CO_2 affinity positively influence the diffusion and solubility parameters that dictate the effectiveness of the gas separation process. Looking forward, outstanding challenges exist in overcoming the complexity that is inter-crystalline growth, which often precludes a MOF from being used in membrane technology.

Mixed-matrix MOF membranes. Although considerable results have been achieved with pure MOF membranes in terms of enhancing selectivity, there remain significant hurdles for attaining satisfactory performance according to industrial standards (that is, combining high permeability and high selectivity). This is primarily because of defects in the membrane from cracks and pinholes and from grain boundary defects, which provide easy lanes for gas molecules to pass through. The incorporation of MOF nanoparticles as a filler within continuous polymer membranes is a technically viable alternative, because the high separation performance of the porous frameworks could then be combined with the satisfactory processability and mechanical stability of polymers.

The first mixed-matrix membrane containing a MOF (Cu BPDC-TED/PAET; TED = triethylenediamine, PAET = poly(3-acetoxyethylthiophene)) was reported in 2004, in which single gas permeation measurements were carried out leading to a CO_2/CH_4 selectivity of 3.2 (REF. 96). There have been many reports since on the use of a wide range of MOF and polymer combinations (Supplementary information (section 3; tables 11,12)). For example, mixed-matrix membranes composed of polyimide and Mg-MOF-74 were fabricated and subjected to gas permeation measurements under conditions relevant for flue gas to assess where the membrane was effective in removing CO_2 (REF. 97). In another study, a ZIF-90/6FDA-DAM (6FDA-DAM = 2,2-bis(3,4-carboxyphenyl) hexafluoropropane dianhydride-diaminomesitylene) mixed-matrix membrane was fabricated and subjected to binary gas permeation measurements (298 K, 2 bar and 1:1 CO_2/CH_4). This mixed-matrix membrane exhibited both enhancement in CO_2 permeability (720 Barrer) and exceptional selectivity ($CO_2/CH_4 = 37$)[98]. Many strategies have been adopted to improve the gas separation properties of mixed-matrix membranes[99], including post-treatment of the membrane[100], post-synthetic modification[101], improving interfacial adhesion between the MOF fillers and polymer[102], as well as modulating the membrane morphology to promote the performance (that is, permselectivity, solubility and diffusivity) to meet industrial standards[103]. However, there are outstanding concerns that remain, including the need to address lower generated permeation from mixed-matrix membranes and solidification, and defect formation as a result of higher MOF loadings.

Reduction and hydrogenation of CO_2

Photocatalytic reduction of CO_2. Low efficiency and yield are the major shortcomings of photocatalytic CO_2 reduction. This process involves multi-electron steps that produce various products, including carbon monoxide, methanol, methane, formaldehyde, formic acid and higher-order hydrocarbons. With the wide range of products that may be formed, there is the challenge of controlling the selectivity for a desired product. Additional challenges include the low solubility of CO_2 if the reaction is performed in aqueous solution as well as the competition of hydrogen generation with CO_2 reduction. A relatively poor understanding of the process and the difficulty in elucidating the mechanisms may make the design of the optimal material challenging.

The first example of photoreduction in MOFs was accomplished with modified UiO-67 (Zr_6O_4 $(OH)_4$(BPYDC); BPYDC = 2,2′-bipyridine-5,5′-dicarboxylate) by replacing the BPDC linker with 4.2 wt% BPYDC linker that had $-Re(CO)_3Cl$ bound to the nitrogen atoms[104] (Supplementary information (section 4; table 13)). This photoactive MOF was used to reduce CO_2 to CO with a turnover number (TON) of 5 in 6 hours and a CO_2/H_2 selectivity of 10. However, this system operated under ultraviolet light, thus others sought to extend photoactivity to the visible light region. The same system of UiO-67 with $-Re(CO)_3Cl$ catalyst bound to the linker was investigated to study the effects of catalyst loading on activity, with a relatively low loading of 13% found to be the optimal amount[105]. The activity was enhanced sevenfold by growing the Re-incorporated MOF on Ag nanocubes to spatially subject the photoactive MOF to intensified electric fields due to surface plasmons[105]. There have also been examples of using Ti- (REF. 106), Fe- (REF. 107), Al- (REF. 108), Cd- (REFS 109,110), Gd- (REF. 111), and Y-based[112] MOFs, in addition to the Co-based ZIF-9 [$Co(bIm)_2$] (REF. 113), sometimes with additional photoactive metal centres.

The most common method for CO_2 reduction to formate also uses Zr-based MOFs, in particular UiO-66 and -67 platforms. The use of UiO-67 modified with a Ru(II) photosensitizer and Mn(I) catalyst grafted onto the linker was shown to reach a similar TON as the previous example of UiO-67 with $-Re(CO)_3Cl$ (REF. 114), although it was less selective for formate production. It is noteworthy that the TON was only reduced by 25% when the CO_2 was diluted to 5% with Ar, with a concomitant drastic improvement in selectivity, thus demonstrating the promise of materials with high selectivity for CO_2. To further exploit the visible light region, the linkers in UiO-66 and -67 were modified to include amino functional groups conjugated with the phenyl ring from the linker. The resulting system absorbs light in the visible region and serves as an antenna for catalytically active metal oxide clusters[115]. Further tuning of these Zr-based MOFs was achieved by combining the amino-functionalized linkers with the post-synthetic incorporation of Ti(IV) instead of Zr(IV)[116,117]. The Ti(IV) cluster has the appropriate redox potential energy to accept electrons from the terephthalate linker. This post-synthetic incorporation of Ti(IV) was done to modify the band structure

of the framework and to use Ti(ɪᴠ) as a mediator for the photoreduction of CO_2 to formate. One of the most active MOFs to date for photoreduction to formate without an additional homogeneous photosensitizer is another Zr-based MOF, NNU-28 ($Zr_6O_4(OH)_4(L)_6$; L = 4,4′-(anthracene-9,10-diylbis(ethyne-2,1-diyl))dibenzoate), which contains an anthracene linker[118]. This structure displayed a TON of 18 over the course of 10 hours under visible light irradiation. This enhanced activity is attributed to the dual catalytic centres of the anthracene linker and the metal oxide cluster that comprise the framework.

Although the majority of photocatalytic products lead to CO or formate, other products have also been shown to form. An Al-based MOF with a Cu-containing porphyrin active centre, Cu-TCPP-$(AlOH)_2$ (TCPP-H_2 = 4,4′,4″,4‴-(porphyrin-5,10,15,20-tetrayl) tetrabenzoate), was used[119], with CH_3OH as the predominant product. The full reduction of CO_2 to CH_4 has also been accomplished photocatalytically following the pyrolysis of Ti-based MIL-125-NH_2 ($Ti_8O_8(OH)_4(BDC-NH_2)_6$) with gold nanoparticles[120]. Finally, a MOF may be used as a composite material, such as with a metal nanoparticle. In this approach, a core–shell motif could be used or the nanoparticles may be bound to the MOF surface. This core–shell material has been achieved with TiO_2 nanoparticles as the shell and HKUST-1 as the core[121]. This construct combines the high selectivity of HKUST-1 for CO_2, improving CO_2 conversion and reducing the production of H_2, with effective charge separation between the nanoparticles and the MOF. Although most studies were performed in the liquid phase, this process is achieved in the gas phase, taking advantage of the high CO_2 uptake of MOF materials.

In summary, the variety of systems used and the products obtained show the versatility and future potential of MOFs for photocatalysis. We have highlighted numerous approaches to improve the photochemical reduction of CO_2. These approaches, which are depicted in FIG. 5, include the use of different SBUs and linkers, grafting the active site onto the linker (and the combination of these two as the source of active sites), and composite materials with nanoparticles. Although a molecular photosensitizer along with a co-catalyst shows the highest activity in terms of TON, it has been possible to design one MOF system containing a photosensitizer as part of the framework with highly selective activity and high TON, thus fully utilizing MOFs as the stand-alone catalytic system with no additives needed.

Electrocatalytic reduction. Electrocatalysis is an alternative means of CO_2 reduction that involves a current applied through a voltage bias. A large overpotential is often used to obtain a substantial yield, which is attributed to the initial formation of the CO_2 radical intermediate before reduction[122], the formation of which has a high activation energy barrier. The challenges in catalyst design are therefore to select a water- and acid-stable catalyst that can operate with a low overpotential to reduce the undesirable hydrogen by-product and enhance selectivity for a particular product from CO_2.

The first report of electrocatalytic CO_2 reduction with a MOF was performed using a Cu(ɪɪ) rubeanate framework containing coordinatively unsaturated metal sites[123]. In this work, formic acid was produced almost exclusively starting from CO_2, with a TON consistently higher than that of a Cu electrode, which was used as a comparison at all applied potentials. This high selectivity was attributed to the relatively weak adsorption of CO_2 to the ionic Cu(ɪɪ) site in the MOF when compared with the adsorption strength of CO_2 to metallic Cu. Despite the high selectivity for the conversion of CO_2, a Faradaic efficiency of only 30% was achieved, with a large amount of H_2 by-product formed. HKUST-1 was also used for CO_2 reduction in DMF[124]. The use of non-aqueous solvent led to the production of oxalic acid with 90% selectivity, which was proposed to occur by dimerization of CO_2. Similar to the previous example, the Faradaic efficiency was relatively low (51%) and the mechanism was attributed to the reduction of Cu(ɪɪ) to Cu(ɪ) followed by electron transfer to the bound CO_2.

The concept of combining the advantages of homogeneous and heterogeneous catalysis is exemplified with the use of a cobalt porphyrin motif linked by 1D aluminium oxide rods [$Al_2(OH)_2$TCPP-Co], with the resulting structure made into a thin film coated on a conductive substrate[125] (FIG. 6). The use of thin film MOFs allows both mass and charge transport to be optimized by controlling the thickness of the films. This maximizes performance through facilitating CO_2 access to the active site while keeping the CO_2 in contact with the electrode at all times. Indeed, selective CO_2 reduction to CO was achieved with a TON of 1,400 over 7 hours and a Faradaic efficiency of 76% in aqueous conditions. It was further shown by spectroelectrochemical studies that Co(ɪɪ) contained within the porphyrin unit was reduced to Co(ɪ) as part of the catalytic cycle.

The thin film MOF approach was extended to iron porphyrin units in MOF-525 [$Zr_6O_4(OH)_4$(TCPP-Fe)$_3$] to effectively concentrate the number of active centres for maximum turnover[126]. The Zr-based framework was found to convert CO_2 to CO in DMF and tetrabutylammonium hexafluorophosphate as the electrolyte with a TON of 272 in just over 4 hours, although H_2 was produced in a 1:1 ratio with CO. Addition of 2,2,2-trifluoroethanol as a weak Brønsted acid increased current densities, leading to a TON of 1,520 over 3.2 hours, again with high H_2 production. The active centre was postulated to be Fe(0), because catalytic currents were noted at more positive potentials than that of the Fe(ɪ/0) redox couple.

Hydrogenation of CO_2 using MOF–nanoparticle composites. Another approach combining Cu nanoparticles with UiO-66 (a 'heterogeneity within order' strategy) has the dual advantage of the MOF protecting the chemically sensitive Cu nanoparticles, and a synergistically enhanced activity. Using this approach, an eightfold increase over the benchmark catalyst and up to 100% selectivity for methanol over CO was recorded[127]. The reason for the high activity was the incorporation of the nanoparticles inside the MOF rather than on the
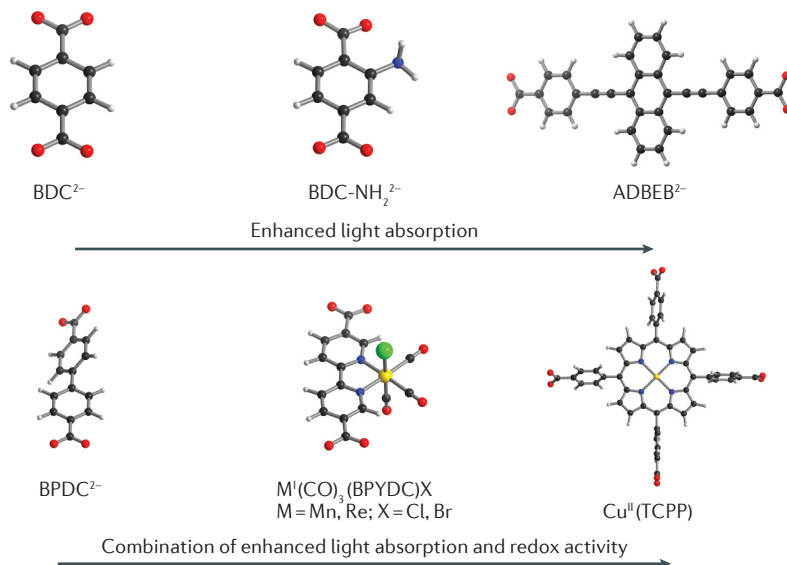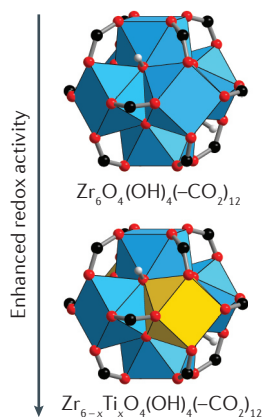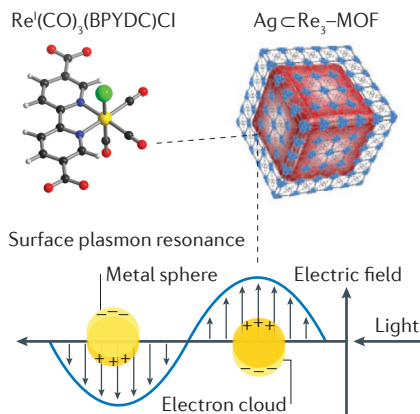
a | Linker-based strategies for improving photophysical properties of MOFs

BDC²⁻

BDC-NH₂²⁻

ADBEB²⁻

Enhanced light absorption

BPDC²⁻

Mᴵ(CO)₃(BPYDC)X
M = Mn, Re; X = Cl, Br

Cuᴵᴵ(TCPP)

Combination of enhanced light absorption and redox activity

b | SBU-based strategies

Zr₆O₄(OH)₄(–CO₂)₁₂

Zr₆₋ₓTiₓO₄(OH)₄(–CO₂)₁₂

Enhanced redox activity

c | 'Heterogeneity within order'

Reᴵ(CO)₃(BPYDC)Cl

Ag⊂Re₃–MOF

Surface plasmon resonance

Metal sphere

Electric field

Light

Electron cloud

Figure 5 | **Strategies for improving photochemical CO₂ reduction.** Photochemical CO₂ reduction performance can be improved by modification of the linker or the secondary building unit (SBU), or by introducing heterogeneity within ordered metal–organic framework (MOF) structures. **a** | Modification of the linker to enhance visible light absorption in successive generations by first incorporating aromatic amines and then anthracene units. Grafting redox active metal centres onto a linker was also explored, first with bipyridine for coordinating Re(ɪ) or Mn(ɪ), and then with porphyrin units chelating Cu(ɪɪ). These modifications lead to augmented light absorption and improved redox activity. **b** | The replacement of Zr(ɪᴠ) with Ti(ɪᴠ) into the Zr₆O₄(OH)₄(–CO₂)₁₂ SBU was investigated for adjusting the energy levels in the band structure of the MOF, resulting in greater redox activity under visible light irradiation. **c** | Optimization of the loading of –Re(CO)₃Cl grafted onto the linker combined with coating a 16 nm MOF thin-film around silver nanoparticles led to an increase in CO₂ photoreduction by an order of magnitude. BDC, terephthalate; BDC-NH₂, 2-aminoterephthalate; ADBEB, 4,4′-(anthracene-9,10-diylbis(ethyne-2,1-diyl))dibenzoate; BPDC, 4,4′-biphenyldicarboxylate; BPYDC, 2,2′-bipyridine-5,5′-dicarboxylate; [TCPP-H₂], 4,4′,4″,4‴-(porphyrin-5,10,15,20- tetrayl) tetrabenzoate. Colour code: C, black; O, red; N, green; Cl or Br, purple; Mn or Re, yellow; Ti, yellow polyhedra; and Zr, blue polyhedra.

surface. A recent extension of this approach came with the use of a UiO-bpy MOF, which anchored Cu/ZnOₓ nanoparticles within the pores to avoid agglomeration[128]. The resulting Cu/ZnOₓ@MOF catalyst achieved high selectivity (100%) and activity (space-time yield of 2.59 $g_{(MeOH)} kg_{(Cu)}^{-1} h^{-1}$) for methanol synthesis from CO₂.

CO₂ conversion for fine chemicals

Chemical exploitation of CO₂ is a parallel development to carbon capture and sequestration that may assist in the reduction of CO₂ emissions. In this scenario, CO₂ is treated as a C1 chemical feedstock for the synthesis of fine chemicals[129,130]. In particular, the synthesis of cyclic organic carbonates through the cycloaddition of CO₂ into epoxides is a primary target for industrial applications.

General considerations. There is a growing number of MOFs that have been utilized as heterogeneous catalysts for the formation of cyclic organic carbonate molecules[131,132] (Supplementary information (section 5; table 15)). In general, the catalytic activity of MOFs arises from three different structural characteristics (FIG. 7). The first is coordinatively unsaturated metals acting as Lewis acidic sites; these are derived from the SBU and/or the linker. In general, such systems require the use of a Lewis basic co-catalyst to be optimally effective. In addition, Lewis basic functionalized linkers can also act as the site of CO₂ fixation. The third characteristic that imparts catalytic activity is Lewis acidic or basic defect sites within the structure or on the surface of the MOF. These catalysts are active even when there is no readily discernible active site available.

Defect-driven catalysis. The earliest reports of MOFs used for the cycloaddition of CO₂ to epoxides were solely based on structural defect sites. Accordingly, MOF-5 was the first MOF used, in which CO₂ was coupled with propylene oxide in the presence of n-Bu₄NBr co-catalyst to form propylene carbonate[133]. The MOF-5/n-Bu₄NBr co-catalyst system led to very high yields of propylene carbonate (97.6%) and was proven to maintain activity over at least three cycles (96% yield in the third cycle). It is worth noting that per cent yields (as opposed to per cent conversion) are often provided for propylene oxide because it is highly volatile (boiling point = 34 °C) and cannot be separated upon CO₂ decompression after the reaction. Although no active site was directly evidenced, the authors showed that both MOF-5 (primary catalyst) and n-Bu₄NBr (co-catalyst) were essential for product formation, because without these the yield significantly decreased. Indeed, given that the Zn₄O SBU is fully saturated, and that defect sites have previously been proposed and reported for this structure[134], catalysis is thought to occur at these imperfections within the crystal structure.

In 2012, ZIF-8 was reported as an effective catalyst in the cycloaddition of CO₂ to epichlorohydrin to form chloropropene carbonate as the main product[135]. As a result of surface defects, derived from strong Lewis acidic Zn(ɪɪ) sites, in addition to the basic nitrogen atoms from the imidazolate linkers, ZIF-8 was demonstrated to be highly active in epichlorohydrin conversion (up to 98.2% at 100 °C) without the need for a co-catalyst or solvent system. To improve the selectivity and yield, ZIF-8 was functionalized on the surface with ethylenediamine (termed ZIF-8-f). This post-synthetic modification technique was successful in increasing the epichlorohydrin conversion to 100% as well as increasing the selectivity
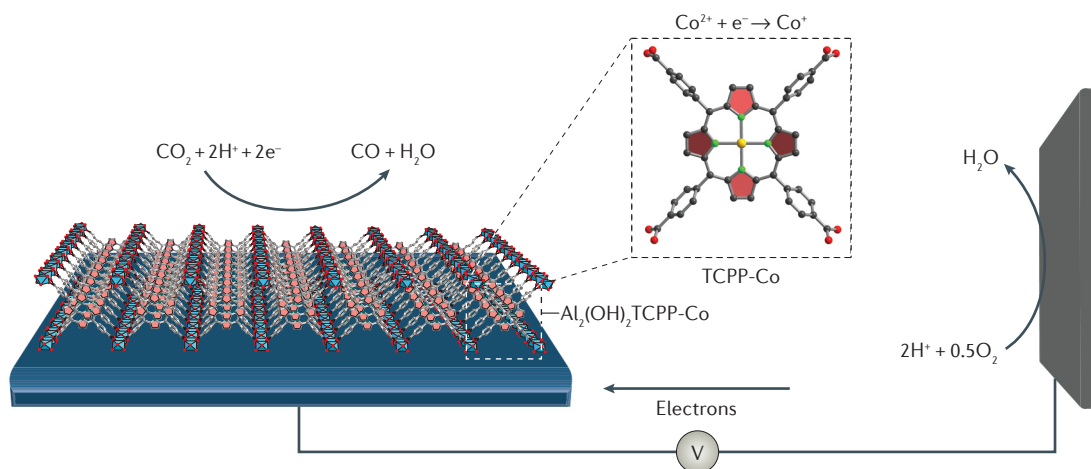
$$CO_2 + 2H^+ + 2e^- \longrightarrow CO + H_2O$$

$$Co^{2+} + e^- \rightarrow Co^+$$

TCPP-Co

$\leftarrow Al_2(OH)_2$TCPP-Co

H_2O

$2H^+ + 0.5O_2$

Electrons

V

Figure 6 | **Electrocatalytic reduction of CO_2 to CO by a Co-porphyrin-containing MOF.** The challenges in designing an electrocatalytically active metal–organic framework (MOF) include the need for a water- and acid-stable material that operates with a low overpotential. Furthermore, the growth and orientation of MOF thin films, which affect the resulting mass and charge transport properties of the material, are crucial for electrochemical applications. Significant success has been achieved by incorporating the advantages of homogeneous electrocatalysts (that is, porphyrin active sites) within a MOF structure (for example, $Al_2(OH)_2$TCPP-Co). The inset shows that the active site is at the metal centre in the porphyrin unit, in this case with Co(II) being reduced to the catalytically active Co(I). [TCPP-H_2], 4,4′,4″,4‴-(porphyrin-5,10,15,20-tetrayl)tetrabenzoate; V, voltage. Colour code: C, black; O, red; N, green; backbone of porphyrin units, light red; and Al, blue polyhedra.

(73.1%) for and yield (73.1%) of chloropropene carbonate at the milder temperature of 80 °C. This report demonstrated that combining strong Lewis acid defect sites at the surface with post-synthetic modification techniques is a beneficial strategy for taking advantage of and enhancing the catalytic performance of MOFs.

Inorganic SBU-driven catalysis. MOF-74 was first used as a catalyst for cyclic organic carbonate synthesis in 2012 (REF. 136). In this report, the Co-MOF-74 structure was shown to effectively catalyse the cycloaddition of CO_2 to styrene oxide (96% conversion) in chlorobenzene without the need for an ammonium co-catalyst under relatively low pressure (20 bar) and temperature (100 °C). The authors pointed out that the conversion decreased as a function of decreasing temperature, which is most likely because of the lower solubility of CO_2 in chlorobenzene. Furthermore, under optimal conditions, this system was recyclable with no loss in conversion percentage over at least three cycles.

The Lewis acidic **gea**-MOF-1 is constructed from tricapped trigonal prismatic $[Y_9(\mu_3\text{-}OH)_8(\mu_2\text{-}OH)_3(O_2C\text{-})_{18}]$ clusters stitched together through the tritopic 1,3,5-benzene(tris)benzoate linker[137]. Because of its exposed Y(III) centres throughout the extended framework, **gea**-MOF-1 was exploited as a heterogeneous catalyst with tetrabutylammonium bromide (TBAB) as a co-catalyst for the cycloaddition of CO_2 and various functionalized epoxides. Under the modest conditions of 120 °C, 20 bar CO_2, **gea**-MOF-1 exhibited high cyclic carbonate product conversions (85–94%) over 6 hours. However, upon comparison with the homogeneous YCl_3/TBAB catalyst system, the **gea**-MOF-1 was found to be ten times less active (turnover frequency of 1,067 hour^{-1} compared with

98 hour^{-1}). Nevertheless, compared with the heterogeneous Y(III)-based analogue Y_2O_3/TBAB, **gea**-MOF-1 led to a greatly increased conversion, TON and frequency.

Linker-promoted catalysis. In 2009, the use of MOF-5 as a catalyst for the cycloaddition of CO_2 to epoxides was further advanced, whereby multivariate (MTV) MOF-5 $[Zn_4O(BDC)_x(BDC\text{-}NH_2)_{3-x}]$ was constructed on the premise that integrating an –NH_2 functionality on the BDC linker would be beneficial in terms of CO_2 fixation and subsequent activation (carbamate intermediate)[138]. Accordingly, the MTV-MOF-5 with 40% BDC-NH_2 incorporation within the structure was found to be an active catalyst alongside tetraethyl ammonium bromide in producing propylene carbonate (63% yield) from CO_2 and propylene oxide. In 2016, a nitrogen-rich triazole linker and Cu-based MOF was synthesized[139]. This MOF featured exposed nitrogen groups in conjunction with Lewis acid Cu(II) catalytic sites — the former for enhancing CO_2 capture and the latter for increasing catalytic activity. Accordingly, the MOF catalyst, with tetra-*n*-butylammonium bromide as a co-catalyst, was shown to be active for the synthesis of various cyclic carbonates under low CO_2 pressure (1 bar) and temperature (25 °C) in a solvent-free environment.

SBU-linker based catalysis. An interesting approach to incorporating both Lewis and Brønsted acid sites within a single framework was recently demonstrated in USTC-253 (Al(OH)(Spbdc); Spbdc = 4,4′-dibenzoic acid-2,2′-sulfone) and its defect-engineered analogue USTC-253-TFA (TFA = trifluoroacetate)[140]. USTC-253 and USTC-253-TFA are isoreticular to elongated MIL-53 (REF. 141) and MOF-253 [Al(OH)(BPYDC)] (REF. 142) with
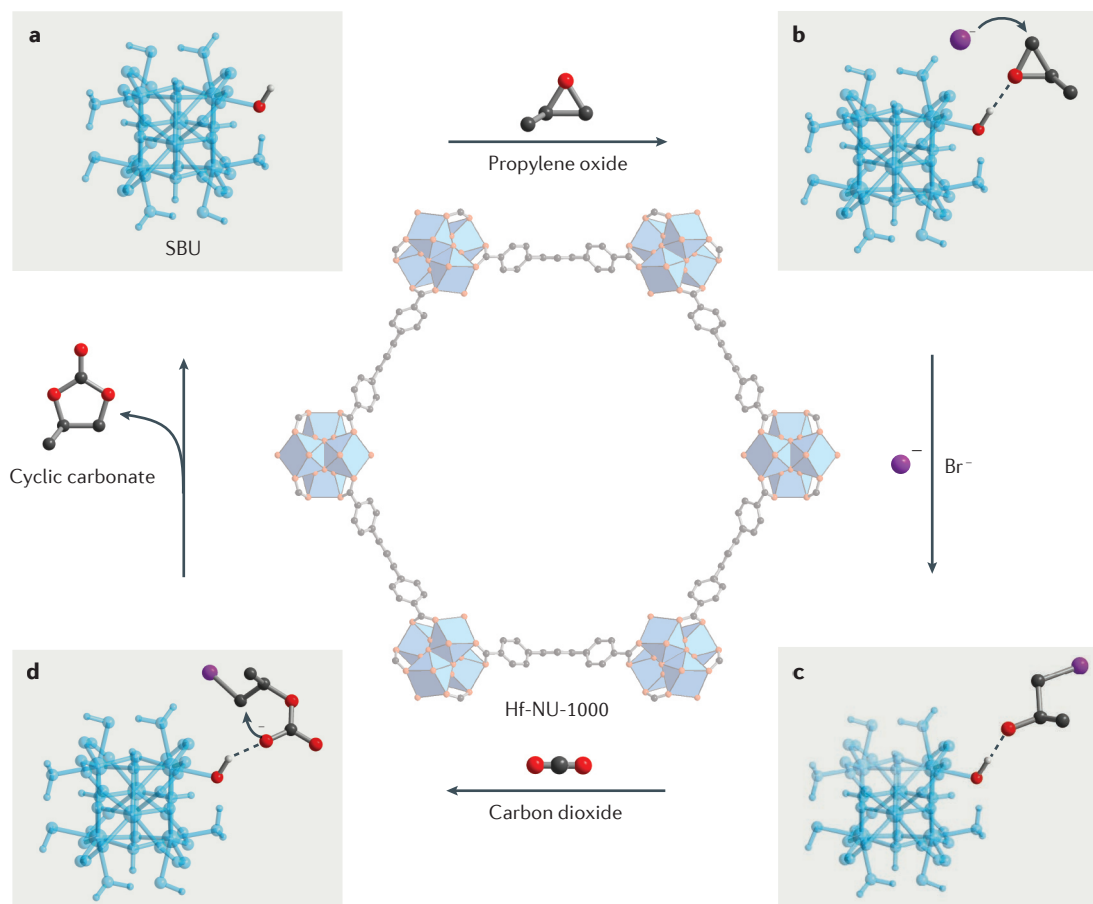
Figure 7 | **Proposed mechanism for the catalytic cycloaddition of propylene oxide with CO_2 by Hf-NU-1000 to form a cyclic carbonate. a,b** | The catalytic nature of Hf-NU-1000 is based on its inorganic secondary building unit (SBU), in which an epoxide (that is, propylene oxide) is bound to a proton from a capping hydroxide ligand[150]. **c** | From there, Br⁻, produced from tetra-*n*-butylammonium bromide, attacks the least sterically hindered carbon of the epoxide to open the ring. **d** | Finally, CO_2 inserts to form an alkylcarbonate anion, which subsequently undergoes ring-closing to form the cyclic carbonate product. Colour code: C, black; O, red; Br, purple; H, white; Hf(IV) ions, blue polyhedra; and Hf-NU-1000 SBU, ball-and-stick inset.

the only difference arising from functionalization of the linker with a sulfone group. The structure is composed of alternating Al(III)–OH chain SBUs and is characterized by the presence of coordinatively unsaturated Al(III) sites lining the pores. Missing linker defects were shown to increase the CO_2 uptake capacity of USTC-253-TFA by 167% as compared to the pristine parent USTC-253. Because of the easily accessible Brønsted (–OH groups in SBUs) and Lewis (coordinatively unsaturated metals) acid sites in conjunction with the increased CO_2 adsorption properties of USTC-253-TFA, cycloaddition reactions of CO_2 to propylene oxide were carried out at room temperature with TBAB as a co-catalyst at a notably low CO_2 pressure of 1 bar. The resulting propylene carbonate was obtained in a higher yield (81.3%) when compared with the defect-free USTC-253 (74.4%).

Recently, it was reported that the isoreticular functionalization of MOF-505 (Cu_2(bptc)(H_2O)$_3$(DMF)$_3$; bptc = 3,3′,5,5′-biphenyltetracarboxylate) with an azomacrocycle-based linker led to the synthesis of a new MOF with **nbo** topology, termed MMCF-2

(Cu_2(Cu-tactmb)(H_2O)$_3$(NO_3)$_2$; tactmb = 1,4,7,10-tetraazacyclododecane-*N*,*N′*,*N″*,*N‴*-tetra-*p*-methyl-benzoate)[143]. By metallating the azomacrocycle *in situ* during the MOF construction, the resulting MMCF-2 framework had a high density of Lewis acid Cu(II) sites. Consequentially, MMCF-2 produced a propylene carbonate yield (95.4%) much higher than that obtained using the non-metallated, isoreticular MOF-505 (48%) under the mild conditions of 1 bar CO_2 and room temperature. The high catalytic activity of MMCF-2 was extended to various substituted epoxides, including butylene oxide, resulting in an 88.5% yield of butylene carbonate under the same conditions. However, when using larger epoxide substrates, the yields of the corresponding cyclic carbonates decreased drastically — a phenomenon that was attributed to size exclusion.

MOFs for this application have reached a level of maturity for molecular catalytic systems with high yields under moderate conditions. The next obvious step is to use CO_2 as a monomer in copolymerization reactions with various epoxides to make commodity polymers.

Indeed, this has been done, albeit in a two-step process, with propylene oxide and CO_2 using HKUST-1 (REF. 144). However, it remains to be seen whether MOFs will be explored over a larger substrate scope or if these materials will be used for other polymerization reactions, including the polymerization of olefins.

Future perspectives

The potential of MOFs for satisfying the demands of every aspect of the CO_2 cycle (TABLE 1) has captured the imagination of scientists, with rapid progress being made in the field, as reflected by the exponentially rising number of publications in this area. With the early phase of discovery and proof-of-concept for CO_2-related applications now well established, the focus of the field is shifting from fundamental aspects to practical considerations. Specifically, the field is increasingly testing materials under conditions applicable to commercial and real-world use, including separation from multiple component mixtures at low concentration and in the presence of water[145], and developing means to recover CO_2 and recycle the MOFs for long-term use.

However, it is important to note that their remains much to be addressed before MOFs for CO_2-related applications are used commercially, as listed in TABLE 1.

Although overcoming the challenge of capturing CO_2 in the presence of water was a big step forward, water is not the only impurity in flue gas, which also contains carbon monoxide, nitrogen oxides and sulfur oxides. Any technology developed for post-combustion CO_2 capture based on MOFs must be able to operate sufficiently and effectively in the presence of these other contaminant molecules. However, there has been little research carried out in this area. Current research movements are centred around testing materials under real conditions with actual flue gas and using a regeneration cycle based on PSA, TSA or VSA, or through the use of membranes. The goal then must be to establish the working capacity of a material in industrially relevant conditions rather than simply assessing the overall uptake. The majority of the foundational work in MOF chemistry has relied on many assumptions, such as static gas uptakes being applicable to dynamic systems, and derived gas selectivities, which make use of single-component isotherms instead of mixtures. The path forward must focus on developing parameters for assessing the performance of MOFs in dynamic settings.

From a structural point of view, targeting MOFs with coordinatively unsaturated metal sites remains a popular research direction. However, considering the

Table 1 | Achievements of MOFs applied to the different components of the CO_2 cycle

Carbon cycle component	Achievements using MOFs	Future directions and challenges
Post-combustion capture	• Tunable structure to improve capture properties • High capacity and selectivity over N_2 • Selective capture in the presence of humidity	• Combine high capacity with high selectivity in the presence of humidity • Assess dynamic adsorption properties in real flue gas streams
Capture in confined spaces	• High capacity at low concentrations (~1% CO_2) • Adsorption occurs in the presence of humidity	• New MOFs with suitable pore walls and environment to improve capacity • Large-scale deployment considerations
Natural gas upgrading	• Tunable pore metrics to improve capture properties • High capacity and selectivity over CH_4 • Selective in the presence of humidity	• Removal of problematic natural gas impurities, notably H_2S • Structural stability towards H_2S
Storage	• Ultrahigh porosities have led to unprecedented capacities	• High cost
Regeneration of MOFs	• Lower energy costs for MOFs in comparison to traditional sorbents • Proof-of-concept achieved with moderate recoveries	• Limited number of MOFs studied for regeneration processes • Benchmark MOFs yet to be studied
MOF-based membranes for separation	• Both pure and mixed-matrix MOF membranes outperform polymeric membranes in terms of permselectivity • Fabrication is mature	• Prevent defects in membrane films • Increase permeation from mixed-matrix membranes • Improve processability
Photocatalytic reduction	• Tunable structures for optimization of bandgaps and light absorption • Accessibility of catalytic active sites • High selectivity achieved for CO and formate	• Increased visible light absorption • Conversion to fully reduced species or higher hydrocarbons • Higher activity • Integration into a flow reactor as opposed to a batch process
Electrocatalytic reduction	• High turnover number with low overpotentials • Moderate selectivity • Properly orientated thin films to maximize mass and charge transport	• Few impactful reports, which are limited to porphyrin-containing MOFs • Thorough understanding of the electrocatalytic process • Conversion to fully reduced species and higher hydrocarbons
Conversion to fine chemicals	• High yields and conversions under moderate conditions for cycloaddition to epoxides • Catalytic structural features identified and readily exploited	• Use CO_2 as monomer for one-step copolymerization reactions with epoxides • Use CO_2 as monomer in copolymerization reactions with olefins

composition of flue gas, this is unlikely to be a successful approach despite the strong CO_2 uptake performance. Instead, heteroatomic frameworks with tailored pore metrics and environments hold the greatest promise for further improving the performance of MOFs under practical conditions. The purpose of controlling the pore metrics and hydrophobicity is to exclude other competing gas molecules, such as water and methane, by maximizing interactions with CO_2. In this regard, combinations of functional groups are an exciting research direction, because the high density of binding sites, when combined with an appropriate pore geometry and environment, could maximize the number of CO_2–framework interactions. To better understand the mechanism of CO_2 capture, it is highly desirable to continue to take advantage of the crystalline nature of MOFs to experimentally probe the structural and chemical changes that occur during CO_2 adsorption and desorption. Indeed, research in this direction has recently yielded some exciting results[71,146–148]. In combination with testing under real-world conditions, a better understanding of this would most certainly help guide future research.

Strong progress has been made in photo- and electrocatalytic CO_2 reduction using MOFs, with new materials being readily designed with improved light absorption, redox chemistry through bandgap tuning, and/or superior conductivity and charge mobility. With several successful catalysts for the selective production of CO and formate, the next step is to move towards the development of a selective MOF catalyst for the controlled production of fully reduced species, such as methane and higher alkanes. Realizing this, in conjunction with the progress made in CO_2 capture and separation, would complete the carbon cycle loop by enabling anthropogenic CO_2 to be captured, purified and recycled as a reusable source of energy. The ultimate goal of CO_2 conversion is slowly being addressed by the flexibility with which catalysts can be designed into MOFs through either molecular means or by encapsulation. It is clear that reticular chemistry, as exemplified by MOFs, will continue to have a major role in providing new, robust materials, especially those with structures that are built from synergistic components, to fully address the CO_2 challenge[149].

1. Furukawa, H., Cordova, K. E., O'Keeffe, M. & Yaghi, O. M. The chemistry and applications of metal-organic frameworks. *Science* **341**, 1230444 (2013).
2. Sumida, K. *et al.* Carbon dioxide capture in metal-organic frameworks. *Chem. Rev.* **112**, 724–781 (2012).
3. Li, J.-R. *et al.* Carbon dioxide capture-related gas adsorption and separation in metal-organic frameworks. *Coord. Chem. Rev.* **255**, 1791–1823 (2011).
4. Jiang, J., Zhao, Y. & Yaghi, O. M. Covalent chemistry beyond molecules. *J. Am. Chem. Soc.* **138**, 3255–3265 (2016).
5. Furukawa, H., Muller, U. & Yaghi, O. M. "Heterogeneity within order" in metal-organic frameworks. *Angew. Chem. Int. Ed.* **54**, 3417–3430 (2015).
6. Millward, A. R. & Yaghi, O. M. Metal-organic frameworks with exceptionally high capacity for storage of carbon dioxide at room temperature. *J. Am. Chem. Soc.* **127**, 17998–17999 (2005).
7. Britt, D., Furukawa, H., Wang, B., Glover, T. G. & Yaghi, O. M. Highly efficient separation of carbon dioxide by a metal-organic framework replete with open metal sites. *Proc. Natl Acad. Sci. USA* **106**, 20637–20640 (2009).
   This publication describes the first breakthrough experiment using MOFs, which is an important method for evaluating CO_2 capture under dynamic conditions.
8. Mason, J. A. *et al.* Application of a high-throughput analyzer in evaluating solid adsorbents for post-combustion carbon capture via multicomponent adsorption of CO_2, N_2, and H_2O. *J. Am. Chem. Soc.* **137**, 4787–4803 (2015).
9. Bao, Z., Yu, L., Ren, Q., Lu, X. & Deng, S. Adsorption of CO_2 and CH_4 on a magnesium-based metal organic framework. *J. Colloid Interface Sci.* **353**, 549–556 (2011).
10. Caskey, S. R., Wong-Foy, A. G. & Matzger, A. J. Dramatic tuning of carbon dioxide uptake via metal substitution in a coordination polymer with cylindrical pores. *J. Am. Chem. Soc.* **130**, 10870–10871 (2008).
11. Märcz, M., Johnsen, R. E., Dietzel, P. D. C. & Fjellvåg, H. The iron member of the CPO-27 coordination polymer series: synthesis, characterization, and intriguing redox properties. *Microporous Mesoporous Mater.* **157**, 62–74 (2012).
12. Yazaydin, A. O. *et al.* Screening of metal-organic frameworks for carbon dioxide capture from flue gas using a combined experimental and modeling approach. *J. Am. Chem. Soc.* **131**, 18198–18199 (2009).
13. Wang, L. J. *et al.* Synthesis and characterization of metal-organic framework-74 containing 2, 4, 6, 8, and 10 different metals. *Inorg. Chem.* **53**, 5881–5883 (2014).
14. Queen, W. L. *et al.* Comprehensive study of carbon dioxide adsorption in the metal-organic frameworks M_2(dobdc) (M = Mg, Mn, Fe, Co, Ni, Cu, Zn). *Chem. Sci.* **5**, 4569–4581 (2014).
15. Kizzie, A. C., Wong-Foy, A. G. & Matzger, A. J. Effect of humidity on the performance of microporous coordination polymers as adsorbents for CO_2 capture. *Langmuir* **27**, 6368–6373 (2011).
16. Si, X. *et al.* High and selective CO_2 uptake, H_2 storage and methanol sensing on the amine-decorated 12-connected MOF CAU-1. *Energy Environ. Sci.* **4**, 4522–4527 (2011).
17. Cui, P. *et al.* Multipoint interactions enhanced CO_2 uptake: a zeolite-like zinc-tetrazole framework with 24-nuclear zinc cages. *J. Am. Chem. Soc.* **134**, 18892–18895 (2012).
18. An, J., Geib, S. J. & Rosi, N. L. High and selective CO_2 uptake in a cobalt adeninate metal-organic framework exhibiting pyrimidine- and amino-decorated pores. *J. Am. Chem. Soc.* **132**, 38–39 (2010).
19. Meyers, A. L. & Prausnitz, J. M. Thermodynamics of mixed-gas adsorption. *AIChE J.* **11**, 121–127 (1965).
20. Hwang, Y. K. *et al.* Amine grafting on coordinatively unsaturated metal centers of MOFs: consequences for catalysis and metal encapsulation. *Angew. Chem. Int. Ed.* **47**, 4144–4148 (2008).
    This paper reported the initial strategy of grafting alkylamines onto MOF structures, thus paving the way for realizing chemisorptive MOF materials.
21. Demessence, A., D'Alessandro, D. M., Foo, M. L. & Long, J. R. Strong CO_2 binding in a water-stable, triazolate-bridged metal-organic framework functionalized with ethylenediamine. *J. Am. Chem. Soc.* **131**, 8784–8786 (2009).
22. McDonald, T. M., D'Alessandro, D. M., Krishna, R. & Long, J. R. Enhanced carbon dioxide capture upon incorporation of *N,N'*-dimethylethylenediamine in the metal-organic framework CuBTTri. *Chem. Sci.* **2**, 2022–2028 (2011).
23. McDonald, T. M. *et al.* Capture of carbon dioxide from air and flue gas in the alkylamine-appended metal-organic framework mmen-Mg_2(dobpdc). *J. Am. Chem. Soc.* **134**, 7056–7065 (2012).
24. Fracaroli, A. M. *et al.* Metal-organic frameworks with precisely designed interior for carbon dioxide capture in the presence of water. *J. Am. Chem. Soc.* **136**, 8863–8866 (2014).
25. Xiong, Y. *et al.* Amide and N-oxide functionalization of T-shaped ligands aford isoreticular MOFs with giant enhancements in CO_2 separation. *Chem. Commun.* **50**, 14631–14634 (2014).
26. Safarifard, V. *et al.* Influence of the amide groups in the CO_2/N_2 selectivity of a series of isoreticular, interpenetrated metal-organic frameworks. *Cryst. Growth Des.* **16**, 6016–6023 (2016).
27. Benson, O. *et al.* Amides do not always work: observation of guest binding in an amide-functionalized porous metal-organic framework. *J. Am. Chem. Soc.* **138**, 14828–14831 (2016).
28. Burd, S. D. *et al.* Highly selective carbon dioxide uptake by [Cu(bpy-*n*)$_2$(SiF$_6$)] (bpy-1 = 4,4'-bipyridine; bpy-2 = 1,2-bis(4-pyridyl)ethene). *J. Am. Chem. Soc.* **134**, 3663–3666 (2012).
29. Nugent, P. *et al.* Porous materials with optimal adsorption thermodynamics and kinetics for CO_2 separation. *Nature* **495**, 80–84 (2013).
30. Liao, P. Q. *et al.* Monodentate hydroxide as a super strong yet reversible active site for CO_2 capture from high-humidity flue gas. *Energy Environ. Sci.* **8**, 1011–1016 (2015).
31. Nguyen, N. T. T. *et al.* Selective capture of carbon dioxide under humid conditions by hydrophobic chabazite-type zeolitic imidazolate frameworks. *Angew. Chem. Int. Ed.* **53**, 10645–10648 (2014).
    This report details the synthesis of hydrophobic ZIFs for selective capture of CO_2 in the presence of water.
32. Ding, N. *et al.* Partitioning MOF-5 into confined and hydrophobic compartments for carbon capture under humid conditions. *J. Am. Chem. Soc.* **138**, 10100–10103 (2016).
33. Zhang, Z. *et al.* Polymer-metal-organic frameworks (polyMOFs) as water tolerant materials for selective carbon dioxide separations. *J. Am. Chem. Soc.* **138**, 920–925 (2016).
34. Liu, B. *et al.* Significant enhancement of gas uptake capacity and selectivity via the judicious increase of open metal sites and Lewis basic sites within two polyhedron-based metal–organic frameworks. *Chem. Commun.* **52**, 3223–3226 (2016).
35. Forrest, K. A., Pham, T., McLaughlin, K., Hogan, A. & Space, B. Insights into an intriguing gas sorption mechanism in a polar MOF with open metal sites and narrow channels. *Chem. Commun.* **50**, 7283–7286 (2014).

36. Li, B. *et al.* Enhanced binding affinity, remarkable selectivity, and high capacity of CO_2 by dual functionalization of a *rht*-type metal-organic framework. *Angew. Chem. Int. Ed.* **51**, 1412–1415 (2012).

37. Kim, J. *et al.* Control of catenation in CuTATB-*n* metal–organic frameworks by sonochemical synthesis and its effect on CO_2 adsorption. *J. Mater. Chem.* **21**, 3070–3076 (2011).

38. Zheng, B., Bai, J., Duan, J., Wojtas, L. & Zaworotko, M. J. Enhanced CO_2 binding affinity of a high-uptake *rht*-type metal-organic framework decorated with acylamide groups. *J. Am. Chem. Soc.* **133**, 758–751 (2011).

39. Lu, Y. *et al.* Porous pcu-type Zn(II) framework material with high adsorption selectivity for CO_2 over N_2. *J. Mol. Struct.* **1107**, 66–69 (2016).

40. Law, J., Watkins, S. & Alexander, D. *In-flight carbon dioxide exposures and related symptoms: associate, susceptibility, and operational implications* (NASA, 2010).

41. Dallbauman, L. A. & Finn, J. E. in *Adsorption and its Applications in Industry and Environmental Protection: Applications in Environmental Protections, Part B* Vol. 120 (ed. Dabrowski, A.) 455–471 (Elsevier, 1999).

42. Bhatt, P. M. *et al.* A fine-tuned fluorinated MOF addresses the needs for trace CO_2 removal and air capture using physisorption. *J. Am. Chem. Soc.* **138**, 9301–9307 (2016).
This contribution describes the first MOF applied towards the capture of a trace amount of CO_2 in confined spaces.

43. Cavenati, S., Grande, C. A. & Rodrigues, A. E. Removal of carbon dioxide from natural gas by vacuum pressure swing adsorption. *Energy Fuels* **20**, 2648–2659 (2006).

44. Ferey, G. *et al.* Why hybrid porous solids capture greenhouse gases? *Chem. Soc. Rev.* **40**, 550–562 (2011).

45. Li, J. R., Sculley, J. & Zhou, H.-C. Metal-organic frameworks for separations. *Chem. Rev.* **112**, 869–832 (2012).

46. Xiong, S. *et al.* A new tetrazolate zeolite-like framework for highly selective CO_2/CH_4 and CO_2/N_2 separation. *Chem. Commun.* **50**, 12101–12104 (2014).

47. Nguyen, N. T. T. *et al.* Mixed-metal zeolitic imidazolate frameworks and their selective capture of wet carbon dioxide over methane. *Inorg. Chem.* **55**, 6201–6207 (2016).

48. Chen, K.-J. *et al.* Tuning pore size in square-lattice coordination networks for size-selective sieving of CO_2. *Angew. Chem. Int. Ed.* **55**, 10268–10272 (2016).

49. Chen, Z. *et al.* Significantly enhanced CO_2/CH_4 separation selectivity within a 3D prototype metal-organic framework functionalized with OH groups on pore surfaces at room temperature. *Eur. J. Inorg. Chem.* **2011**, 2227–2231 (2011).

50. Bae, Y.-S. *et al.* Separation of CO_2 from CH_4 using mixed-ligand metal-organic frameworks. *Langmuir* **24**, 8592–8598 (2008).

51. Hamon, L. *et al.* Comparative study of hydrogen sulfide adsorption in the MIL-53(Al, Cr, Fe), MIL-47(V), MIL-100(Cr), and MIL-101(Cr) metal-organic frameworks at room temperature. *J. Am. Chem. Soc.* **131**, 8775–8777 (2009).

52. Hamon, L. *et al.* Molecular insight into the adsorption of H_2S in the flexible MIL-53(Cr) and rigid MIL-47(V) MOFs: Infrared spectroscopy combined to molecular simulations. *J. Phys. Chem. C* **115**, 2047–2056 (2011).

53. Belmabkhout, Y. *et al.* Metal-organic frameworks to satisfy gas upgrading demands: fine-tuning the soc-MOF platform for the operative removal of H_2S. *J. Mater. Chem. A* **5**, 3293–3303 (2017).

54. Vellingiri, K., Deep, A. & Kim, K.-H. Metal-organic frameworks as a potential platform for selective treatment of gaseous sulfur compounds. *ACS Appl. Mater. Interfaces* **8**, 29835–29857 (2016).

55. Gedrich, K. *et al.* A highly porous metal-organic framework with open nickel sites. *Angew. Chem. Int. Ed.* **49**, 8489–8492 (2010).

56. Alezi, D. *et al.* MOF crystal chemistry paving the way to gas storage needs: aluminum-based soc-MOF for CH_4, O_2, and CO_2 storage. *J. Am. Chem. Soc.* **137**, 13308–13318 (2015).

57. Yuan, D., Zhao, D., Sun, D. & Zhou, H. C. An isoreticular series of metal-organic frameworks with dendritic hexacarboxylate ligands and exceptionally high gas-uptake capacity. *Angew. Chem. Int. Ed.* **49**, 5357–5361 (2010).

58. Xue, M. *et al.* New prototype isoreticular metal-organic framework $Zn_4O(FMA)_3$ for gas storage. *Inorg. Chem.* **48**, 4649–4651 (2009).

59. Farha, O. K. *et al. De novo* synthesis of a metal-organic framework material featuring ultrahigh surface area and gas storage capacities. *Nat. Chem.* **2**, 944–948 (2010).

60. Dietzel, P. D. C., Besikiotis, V. & Blom, R. Application of metal–organic frameworks with coordinatively unsaturated metal sites in storage and separation of methane and carbon dioxide. *J. Mater. Chem.* **19**, 7362–7370 (2009).

61. Llewellyn, P. L. *et al.* High uptakes of CO_2 and CH_4 in mesoporous metal-organic frameworks MIL-100 and MIL-101. *Langmuir* **24**, 7245–7250 (2008).

62. Furukawa, H. *et al.* Ultrahigh porosity in metal-organic frameworks. *Science* **329**, 424–428 (2010).
This report details the synthesis of ultra-highly porous MOFs, using the principles of reticular chemistry, which resulted in record-breaking CO_2 uptake properties.

63. Mason, J. A., Sumida, K., Herm, Z. R., Krishna, R. & Long, J. R. Evaluating metal-organic frameworks for post-combustion carbon dioxide capture *via* temperature swing adsorption. *Energy Environ. Sci.* **4**, 3030–3040 (2011).
This publication demonstrated the feasibility of regenerating MOFs through temperature swing adsorption processes.

64. Olajire, A. A. CO_2 capture and separation technologies for end-of-pipe applications — a review. *Energy* **35**, 2610–2628 (2010).

65. Yu, C.-H., Huang, C.-H. & Tan, C.-S. A review of CO_2 capture by absorption and adsorption. *Aerosol Air Qual. Res.* **12**, 745–769 (2012).

66. Sircar, S. & Golden, T. C. Purification of hydrogen by pressure swing adsorption. *Sep. Sci. Technol.* **35**, 667–687 (2000).

67. Herm, Z. R., Swisher, J. A., Smit, B., Krishna, R. & Long, J. R. Metal-organic frameworks as adsorbents for hydrogen purification and precombustion carbon dioxide capture. *J. Am. Chem. Soc.* **133**, 5664–5667 (2011).

68. Ferreira, A. F. P., Ribeiro, A. M., Kulaç, S. & Rodrigues, A. E. Methane purification by adsorptive processes on MIL-53(Al). *Chem. Eng. Sci.* **124**, 79–95 (2015).

69. Serra-Crespo, P. *et al.* Preliminary design of a vacuum pressure swing adsorption process for natural gas upgrading based on amino-functionalized MIL-53. *Chem. Eng. Technol.* **38**, 1183–1194 (2015).

70. Berger, A. H. & Bhown, A. S. Comparing physisorption and chemisorption solid sorbents for use separating CO_2 from flue gas using temperature swing adsorption. *Energy Procedia* **4**, 562–567 (2011).

71. McDonald, T. M. *et al.* Cooperative insertion of CO_2 in diamine-appended metal-organic frameworks. *Nature* **519**, 303–308 (2015).
This work highlights an alternative CO_2 capture mechanism for an alkylamine-appended MOF to the established aqueous monoethanolamine system, indicating solid-state systems may operate differently despite both being chemisorptive processes.

72. Ye, S. *et al.* Post-combustion CO_2 capture with the HKUST-1 and MIL-101(Cr) metal-organic frameworks: adsorption, separation and regeneration investigations. *Microporous Mesoporous Mater.* **179**, 191–197 (2013).

73. Dasgupta, S. *et al.* CO_2 recovery from mixtures with nitrogen in a vacuum swing adsorber using metal-organic framework adsorbent: a comparative study. *Int. J. Greenh. Gas Control* **7**, 225–229 (2012).

74. Andersen, A. *et al.* On the development of vacuum swing adsorption (VSA) technology for post-combustion CO_2 capture. *Energy Procedia* **37**, 33–39 (2013).

75. Zhang, Y., Sunarso, J., Liu, S. M. & Wang, R. Current status and development of membranes for CO_2/CH_4 separation: A review. *Int. J. Greenhouse Gas Control* **12**, 84–107 (2013).

76. Robeson, L. M. Correlation of separation factor versus permeability for polymeric membranes. *J. Membr. Sci.* **62**, 165–185 (1991).

77. Rui, Z., James, J. B., Kasik, A. & Lin, Y. S. Metal-organic framework membrane process for high purity CO_2 production. *AIChE J.* **62**, 3836–3841 (2016).

78. Robeson, L. M. The upper bound revisited. *J. Membr. Sci.* **320**, 390–400 (2008).

79. Koros, W. J. & Mahajan, R. Pushing the limits on possibilities for large scale gas separation: which strategies? *J. Membr. Sci.* **181**, 141 (2001).

80. Venna, S. R. & Carreon, M. A. Metal-organic framework membranes for carbon dioxide separation. *Chem. Eng. Sci.* **124**, 3–19 (2015).

81. Hermes, S., Schroder, F., Chelmowski, R., Woll, C. & Fischer, R. A. Selective nucleation and growth of metal-organic open framework thin films on patterned $COOH/CF_3$-terminated self-assembled monolayers on Au(111). *J. Am. Chem. Soc.* **127**, 13744–13745 (2005).
This contribution details the growth of the first pure MOF membrane, which serves as the basis for later developments in using MOF membranes for gas separations.

82. Liu, Y. Synthesis of continuous MOF-5 membranes on porous α-alumina substrates. *Microporous Mesoporous Mater.* **118**, 296–301 (2009).

83. Qiu, S., Xue, M. & Zhu, G. Metal-organic framework membranes: from synthesis to separation application. *Chem. Soc. Rev.* **43**, 6116–6140 (2014).

84. Liu, Y. *et al.* Remarkable enhanced gas separation by partial self-conversion of a laminated membrane to metal-organic frameworks. *Angew. Chem. Int. Ed.* **54**, 3028–3032 (2015).

85. Peng, Y. *et al.* Metal-organic framework nanosheets as building blocks for molecular sieving membranes. *Science* **346**, 1356–1359 (2014).

86. Liu, Y., Zeng, G., Pan, Y. & Lai, Z. Synthesis of highly *c*-oriented ZIF-69 membranes by secondary growth and their gas permeation properties. *J. Membr. Sci.* **379**, 46–51 (2011).

87. Liu, Y., Hu, E. P., Khan, E. A. & Lai, Z. Synthesis and characterization of ZIF-69 membranes and separation for CO_2/CO mixture. *J. Membr. Sci.* **353**, 36–40 (2010).

88. An, J., Fiorella, R., Geib, S. J. & Rosi, N. L. Synthesis, structure, assembly, and modulation of the CO_2 adsorption properties of a zinc-adeninate macrocyle. *J. Am. Chem. Soc.* **131**, 8401–8403 (2009).

89. Bohrman, J. A. & Carreon, M. A. Synthesis and CO_2/CH_4 separation performance of bio-MOF-1 membranes. *Chem. Commun.* **48**, 5130–5132 (2012).

90. Xie, Z., Li, T., Rosi, N. L. & Carreon, M. A. Alumina-supported cobalt-adeninate MOF membranes for CO_2/CH_4 separation. *J. Mater. Chem. A* **2**, 1239–1241 (2014).

91. Al-Maythalony, B. A. *et al.* Quest for anionic MOF membranes: continuous sod-ZMOF membrane with CO_2 adsorption-driven selectivity. *J. Am. Chem. Soc.* **137**, 1754–1757 (2015).

92. Bétard, A. *et al.* Fabrication of a CO_2-selective membrane by stepwise liquid-phase deposition of an alkylether functionalized pillared-layered metal-organic framework $[Cu_2L_3P]_n$ on a macroporous support. *Microporous Mesoporous Mater.* **150**, 76–82 (2012).

93. Huang, A., Liu, Q., Wang, N. & Caro, J. Organosilica functionalized zeolitic imidazolate framework ZIF-90 membrane for CO_2/CH_4 separation. *Microporous Mesoporous Mater.* **192**, 18–22 (2014).

94. Zhao, Z., Ma, X., Kasik, A., Li, Z. & Lin, Y. S. Gas separation properties of metal organic framework (MOF-5) membranes. *Ind. Eng. Chem. Res.* **52**, 1102–1108 (2013).

95. Yin, H. *et al.* A highly permeable and selective amino-functionalized MOF CAU-1 membrane for CO_2-N_2 separation. *Chem. Commun.* **50**, 3699–3701 (2014).

96. Yehia, H., Pisklak, T. J., Ferraris, J. P., Balkus, K. J. & Musselman, I. H. Methane facilitated transport using copper(II) biphenyl dicarboxylate-triethylenediamine poly(3-acetoxyethylthiophene) mixed matrix membranes. *Polym. Preprints* **45**, 35–36 (2004).

97. Bae, T.-H. & Long, J. R. CO_2/N_2 separation with mixed-matrix membranes containing $Mg_2(dobdc)$ nanocrystals. *Energy Environ. Sci.* **6**, 3565–3569 (2013).

98. Bae, T.-H. *et al.* A high-performance gas-separation membrane containing submicrometer-sized metal-organic framework crystals. *Angew. Chem. Int. Ed.* **49**, 9863–9866 (2010).

99. Seoane, B. *et al.* Metal-organic framework based mixed matrix membranes: a solution for highly efficient CO_2 capture? *Chem. Soc. Rev.* **44**, 2421–2454 (2015).

100. Duan, C., Ji, X., Liu, D., Cao, Y. & Yuan, Q. Post-treatment effect on gas separation property of mixed matrix membranes containing metal organic frameworks. *J. Membr. Sci.* **466**, 92–102 (2014).

101. Al-Maythalony, B. *et al.* Tuning the interplay between selectivity and permeability of ZIF-7 mixed matrix membranes. *ACS Appl. Mater. Interfaces* http://dx.doi.org/10.1021/acsami.6b15803 (2017). **This contribution details a post-synthetic modification strategy to fine-tune the permselectivity of spongy mixed matrix membranes.**

102. Wang, Z., Wang, D., Zhang, S., Hu, L. & Jin, J. Interfacial design of mixed matrix membranes for improved gas separation performance. *Adv. Mater.* **28**, 3399–3405 (2016).

103. Zhang, C. *et al.* Highly scalable ZIF-based mixed-matrix hollow fiber membranes for advanced hydrocarbon separations. *AIChE J.* **60**, 2625–2635 (2014).

104. Wang, C., Xie, Z., DeKrafft, K. E. & Lin, W. Doping metal-organic frameworks for water oxidation, carbon dioxide reduction, and organic photocatalysis. *J. Am. Chem. Soc.* **133**, 13445–13454 (2011).

105. Choi, K. *et al.* Plasmon-enhanced photocatalytic CO_2 conversion within metal-organic frameworks under visible light. *J. Am. Chem. Soc.* **139**, 356–362 (2017). **This publication details the use of a 'heterogeneity within order' strategy for constructing a highly active photocatalytic MOF used for CO_2 conversion to CO.**

106. Fu, Y. *et al.* An amine-functionalized titanium metal-organic framework photocatalyst with visible-light-induced activity for CO_2 reduction. *Angew. Chem. Int. Ed.* **51**, 3364–3367 (2012).

107. Wang, D., Huang, R., Liu, W., Sun, D. & Li, Z. Fe-based MOFs for photocatalytic CO_2 reduction: role of coordination unsaturated sites and dual excitation pathways. *ACS Catal.* **4**, 4254–4260 (2014).

108. Sun, D. *et al.* Construction of a supported Ru complex on bifunctional MOF-253 for photocatalytic CO_2 reduction under visible light. *Chem. Commun.* **51**, 2645–2648 (2015).

109. Zhang, S. *et al.* Hierarchical metal–organic framework nanoflowers for effective CO_2 transformation driven by visible light. *J. Mater. Chem. A* **3**, 15764–15768 (2015).

110. Zhang, S., Li, L., Zhao, S., Sun, Z. & Luo, J. Construction of interpenetrated ruthenium metal–organic frameworks as stable photocatalysts for CO_2 reduction. *Inorg. Chem.* **54**, 8375–8379 (2015).

111. Wu, P. *et al.* Photoactive metal – organic framework and its film for light-driven hydrogen production and carbon dioxide reduction. *Inorg. Chem.* **55**, 8153–8159 (2016).

112. Li, L. *et al.* Effective visible-light driven CO_2 photoreduction *via* a promising bifunctional iridium coordination polymer. *Chem. Sci.* **5**, 3808–3813 (2014).

113. Wang, S., Yao, W., Lin, J., Ding, Z. & Wang, X. Cobalt imidazolate metal-organic frameworks photosplit CO_2 under mild reaction conditions. *Angew. Chem. Int. Ed.* **53**, 1034–1038 (2014).

114. Fei, H., Sampson, M. D., Lee, Y., Kubiak, C. P. & Cohen, S. M. Photocatalytic CO_2 reduction to formate using a Mn(I) molecular catalyst in a robust metal-organic framework. *Inorg. Chem.* **54**, 6821–6828 (2015).

115. Sun, D. *et al.* Studies on photocatalytic CO_2 reduction over NH_2-UiO-66(Zr) and its derivatives: towards a better understanding of photocatalysis on metal-organic frameworks. *Chem. Eur. J.* **19**, 14279–14285 (2013).

116. Lee, Y., Kim, S., Kang, J. K. & Cohen, S. M. Photocatalytic CO_2 reduction by a mixed metal (Zr/Ti), mixed ligand metal-organic framework under visible light irradiation. *Chem. Commun.* **51**, 5735–5738 (2015).

117. Sun, D., Liu, W., Qiu, M., Zhang, Y. & Li, Z. Introduction of a mediator for enhancing photocatalytic performance *via* post-synthetic metal exchange in metal-organic frameworks (MOFs). *Chem. Commun.* **51**, 2056–2059 (2015).

118. Chen, D., Xing, H., Wang, C. & Su, Z. Highly efficient visible-light-driven CO_2 reduction to formate by a new anthracene-based zirconium MOF *via* dual catalytic routes. *J. Mater. Chem. A* **4**, 2657–2662 (2016).

119. Liu, Y. *et al.* Chemical adsorption enhanced CO_2 capture and photoreduction over a copper porphyrin based metal-organic framework. *ACS Appl. Mater. Interfaces* **5**, 7654–7658 (2013).

120. Khaletskaya, K. *et al.* Fabrication of gold/titania photocatalyst for CO_2 reduction based on pyrolytic conversion of the metal-organic framework NH_2-MI-125(Ti) loaded with gold nanoparticles. *Chem. Mater.* **27**, 7248–7257 (2015).

121. Li, R. *et al.* Integration of an inorganic semiconductor with a metal-organic framework: a platform for enhanced gaseous photocatalytic reactions. *Adv. Mater.* **26**, 4783–4788 (2014).

122. Li, W. in *Advances in CO_2 Conversion and Utilization* (ed. Hu, Y. H.) 55–76 (American Chemical Society, 2010).

123. Hinogami, R. *et al.* Electrochemical reduction of carbon dioxide using a copper rubeanate metal-organic framework. *ECS Electrochem. Lett.* **1**, H17–H19 (2012).

124. Senthil Kumar, R., Senthil Kumar, S. & Anbu Kulandainathan, M. Highly selective eletrochemical reduction of carbon dioxide using Cu-based metal-organic framework as an electrocatalyst. *Electrochem. Commun.* **25**, 70–73 (2012).

125. Kornienko, N. *et al.* Metal-organic frameworks for electrocatalytic reduction of carbon dioxide. *J. Am. Chem. Soc.* **137**, 14129–14135 (2015).

126. Hod, I. *et al.* Fe-porphyrin-based metal-organic framework films as high-surface concentration, heterogeneous catalysts for electrochemical reduction of CO_2. *ACS Catal.* **5**, 6302–6309 (2015). **This electrocatalytic system makes use of a highly active molecular catalyst as the linker for MOF synthesis. The resulting thin films lead to maximal mass and charge transport for CO_2 reduction.**

127. Rungtaweevoranit, B. *et al.* Copper nanocrystals encapsulated in Zr-based metal-organic frameworks for highly selective CO_2 hydrogenation to methanol. *Nano Lett.* **16**, 7645–7649 (2016). **This contribution is the first report of a MOF used for hydrogenation of CO_2 to a liquid fuel.**

128. An, B. *et al.* Confinement of ultrasmall Cu/ZnO$_x$ nanoparticles in metal-organic frameworks for selective methanol synthesis from catalytic hydrogenation of CO_2. *J. Am. Chem. Soc.* **139**, 3834–3840 (2017).

129. Aresta, M., Dibenedetto, A. & Angelini, A. Catalysis for the valorization of exhaust carbon: from CO_2 to chemicals, materials, and fuels. Technological use of CO_2. *Chem. Rev.* **114**, 1709–1742 (2014).

130. Sakakura, T., Choi, J.-C. & Yasuda, H. Transformation of carbon dioxide. *Chem. Rev.* **107**, 2365–2387 (2007).

131. Beyzavi, M. H. *et al.* Metal-organic framework-based catalysts: chemical fixation of CO_2 with epoxides leading to cyclic organic carbonates. *Front. Energy Res.* **2**, 63 (2015).

132. He, H., Perman, J. A., Zhu, G. & Ma, S. Metal-organic frameworks for CO_2 chemical transformations. *Small* **12**, 6309–6324 (2016).

133. Song, J. *et al.* MOF-5/*n*-Bu$_4$Br: an efficient catalyst system for the synthesis of cyclic carbonates from epoxides and CO_2 under mild conditions. *Green Chem.* **11**, 1031–1036 (2009).

134. Rayon, U. *et al.* Engineering of coordination polymers for shape selective alkylation of large aromatics and the role of defects. *Microporous Mesoporous Mater.* **129**, 319–329 (2010).

135. Miralda, C. M., Macias, E. E., Zhu, M., Ratnasamy, P. & Carreon, M. A. Zeolitic imidazolate framework-8 catalysts in the conversion of CO_2 to chloropropene carbonate. *ACS Catal.* **2**, 180–183 (2012).

136. Cho, H.-Y., Yang, D.-A., Kim, J., Jeong, S.-Y. & Ahn, W.-S. CO_2 adsorption and catalytic application of Co-MOF-74 synthesized by microwave heating. *Catal. Today* **185**, 35–40 (2012).

137. Guillerm, V. *et al.* Discovery and introduction of a (3,18)-connected net as an ideal blueprint for the design of metal-organic frameworks. *Nat. Chem.* **6**, 673–680 (2014).

138. Kleist, W., Jutz, F., Maciejewski, M. & Baiker, A. Mixed-linker metal-organic frameworks as catalysts for the synthesis of propylene carbonate from propylene oxide and CO_2. *Eur. J. Inorg. Chem.* **2009**, 3552–3561 (2009).

139. Li, P.-Z. *et al.* A triazole-containing metal-organic framework as a highly effective and substrate size-dependent catalyst for CO_2 conversion. *J. Am. Chem. Soc.* **138**, 2142–2145 (2016).

140. Jiang, Z.-R., Wang, H., Hu, Y., Lu, J. & Jiang, H.-L. Polar group and defect engineering in a metal-organic framework: synergistic promotion of carbon dioxide sorption and conversion. *ChemSusChem* **8**, 878–885 (2015).

141. Senkovska, I. *et al.* New highly porous aluminium based metal-organic frameworks: Al(OH)(ndc) (ndc = 2,6-naphthalene dicarboxylate) and Al(OH)(bpdc) (bpdc = 4,4'-biphenyl dicarboxylate) *Microporous Mesoporous Mater.* **122**, 93–98 (2009).

142. Bloch, E. D. *et al.* Metal insertion in a microporous metal-organic framework lined with 2,2'-bipyridine. *J. Am. Chem. Soc.* **132**, 14382–14384 (2010).

143. Gao, W.-Y. *et al.* Crystal engineering of an nbo topology metal-organic framework for chemical fixation of CO_2 under ambient conditions. *Angew. Chem. Int. Ed.* **53**, 2615–2619 (2014).

144. Darensbourg, D. J., Chung, W.-C., Wang, K. & Zhou, H.-C. Sequestering CO_2 for short-term storage in MOFs: copolymer synthesis with oxiranes. *ACS Catal.* **4**, 1511–1515 (2014).

145. González-Zamora, E. & Ibarra, I. A. CO_2 capture under humid conditions in metal-organic frameworks. *Mater. Chem. Front.* http://dx.doi.org/10.1039/c6qm00301j (2017).

146. Drisdell, W. S. *et al.* Probing the mechanism of CO_2 capture in diamine-appended metal-organic frameworks using measured and simulated X-ray spectroscopy. *Phys. Chem. Chem. Phys.* **17**, 21448–21457 (2015).

147. Queen, W. L. *et al.* Site-specific CO_2 adsorption and zero thermal expansion in an isotropic pore network. *J. Phys. Chem. C* **115**, 24915–24919 (2011).

148. Lee, J. S. *et al.* Understanding small-molecule interactions in metal-organic frameworks: coupling experiment with theory. *Adv. Mater.* **27**, 5785–5796 (2015).

149. Schoedel, A., Ji, Z. & Yaghi, O. M. The role of metal-organic frameworks in a carbon-neutral energy cycle. *Nat. Energy* **1**, 16034 (2016).

150. Hassan Beyzavi, M. *et al.* A hafnium-based metal-organic framework as an efficient and multifunctional catalyst for facile CO_2 fixation and regioselective and enantioretentive epoxide activation. *J. Am. Chem. Soc.* **136**, 15861–15864 (2014).

Publisher's note
Springer Nature remains neutral with regard to jurisdictional claims in published maps and institutional affiliations.

How to cite this article
Trickett, C. A. *et al.* The chemistry of metal–organic frameworks for CO_2 capture, regeneration and conversion. *Nat. Rev. Mater.* **2**, 17045 (2017).

SUPPLEMENTARY INFORMATION
See online article: S1 (tables)
ALL LINKS ARE ACTIVE IN THE PDF